

2015

Aggregation of Squaraine Dye Derivatives in Solid State Spin-coated Thin Films

Mohammed Daoudi
University of Central Florida

 Part of the [Chemistry Commons](#)

Find similar works at: <https://stars.library.ucf.edu/etd>

University of Central Florida Libraries <http://library.ucf.edu>

This Doctoral Dissertation (Open Access) is brought to you for free and open access by STARS. It has been accepted for inclusion in Electronic Theses and Dissertations, 2004-2019 by an authorized administrator of STARS. For more information, please contact STARS@ucf.edu.

STARS Citation

Daoudi, Mohammed, "Aggregation of Squaraine Dye Derivatives in Solid State Spin-coated Thin Films" (2015). *Electronic Theses and Dissertations, 2004-2019*. 1210.
<https://stars.library.ucf.edu/etd/1210>

AGGREGATION OF SQUARINE DYE DERIVATIVES IN SOLID STATE SPIN COATED THIN FILMS

by

MOHAMMED DAOUDI
B.S. University of Damascus, 1976
M.S. University of Central Florida, 2005

A dissertation submitted in partial fulfillment of the requirements
for the degree of Doctor of Philosophy
in the Department of Chemistry
in the College of Sciences
at the University of Central Florida
Orlando, Florida

Summer Term
2015

Major Professor: Kevin D. Belfield

©2015 Mohammed Daoudi

ABSTRACT

Squaraine dyes have been the subject of intensive studies due their unusual electronic properties that make them good candidates for a wide range of applications in various technological fields. They are particularly promising in nonlinear optics, bioimaging for labeling and sensing of biomolecules, as sensitizers for solar energy harvesting in solar cells and organic photovoltaics, two-photon absorbing materials, near-infrared (NIR) emitting fluorescent probes, second harmonic generation organic dyes, and sensitizers for photodynamic therapy among others.

In this dissertation, the aggregation behaviors and features of several squaraine dye derivatives in solid state thin films were studied and reported.

In the first chapter of the dissertation, three squaraine dye derivatives with two and four hydroxy groups and with different N-alkyl amino donor substituents were synthesized and used as models to study aggregation behavior. Their UV-vis absorption, thermal properties, and photoluminescence properties were determined. The models with four hydroxy substituents exhibited higher thermal stability and melt at higher temperature compared to the dye with only two hydroxy substituents due to increased hydrogen bonding. The UV-vis absorption and photoluminescence properties in liquid solution at room temperature were found to be similar.

In the second chapter, the squaraine dyes, 2,4-bis [4-(N,N-di-n-pentylamino)-2-hydroxyphenyl] squaraine [SQC5(OH)₂], 2,4-bis [4-(N,N-di-n-pentylamino)-2,4-hydroxyphenyl] squaraine [SQC5(OH)_{4 n}], and 2,4-bis [4-(N,N-di-isopentylamino)-2,4-hydroxyphenyl] squaraine [SQC5(OH)_{4 b}], where “n” and “b” stand for normal or linear and branched alkyl groups, respectively, were investigated to study their aggregation in solid state thin film form using UV-vis absorption spectroscopy. The investigation revealed significant differences in aggregation behaviors and features.

The dye SQC5(OH)₂ mainly exhibited J-type aggregation with an intense absorption band in the NIR region. In contrast, the SQC5(OH)_{4 n} and SQC5(OH)_{4 b} compounds mainly exhibited H-type aggregation, characterized by less intense and blue shifted absorption bands.

The third chapter presents the kinetic study conducted on the squaraine dye derivative 2,4-bis [4-(N,N-di-n-pentylamino)-2-hydroxyphenyl] squaraine [SQC5(OH)₂] in solid state spin-coated thin films. The study revealed the formation of J-aggregates with bands at 767 nm at room temperature. This aggregate was temperature dependent. It was transformed into H-aggregates as the temperature increased. The activation energy of the decay (transformation) process was found to be 91.2 kJ. The values of ΔH and ΔS are 88.4 kJ/mol and 48.2 J/K.mol, respectively, indicating the J-aggregate of SQC5(OH)₂ was a kinetic product while the H-aggregate was thermodynamically more stable.

I dedicate this dissertation to my family

ACKNOWLEDGMENTS

I would like to express my sincere gratitude to my major research advisor Dr. Kevin D. Belfield for his constant encouragement, inspiration, support, patience, and advises throughout the course of this work.

I am highly grateful to the members of my dissertation committee, Dr. Howard Miles, Dr. Andreas Campiglia, Dr. Aniket Bhattacharya, and Dr. Matthew Rex for their valuable discussion and support and for their time to evaluate my dissertation.

I would like to thank the Department of Chemistry at University of Central Florida for giving me the opportunity to do my graduate study.

I have received many valuable and helpful suggestions and ideas from all the fellow graduate students and post docs in our group. I would like to thank them all for friendly and cooperative environment.

TABLE OF CONTENT

LIST OF FIGURES	x
LIST OF TABLES	xii
LIST OF SCHEMES	xiii
LIST OF ACRONYMS AND ABBREVIATIONS	xiv
CHAPTER 1 : SQUARINE DERIVATIVES SYNTHESIS AND CHARACTERIZATION	1
1.1 Abstract	1
1.2 Introduction	1
1.3 Experimental Section	2
1.3.1 Squaraine dyes preparation	2
1.3.2 Thermal Characterization	6
1.3.3 Photophysical Characterization	6
1.4 Results and Discussion	7
1.5 Conclusion	11
CHAPTER 2 : INVESTIGATION OF SQUARINE DERIVATIVES AGGREGATION IN SOLID STATE SPIN-COATED THIN FILMS	12
2.1 Abstract	12
2.2 Introduction	12
2.3 Experimental Section	17

2.3.1	Spectroscopic Measurements	17
2.3.2	Preparation of the Spin-coated Films	17
2.3.3	Photoluminescence Measurements	18
2.3.4	Thin Film X-ray Diffraction Measurements	18
2.4	Results and Discussion.....	18
2.5	Conclusion.....	28
CHAPTER 3 : KINETIC INVESTIGATION OF THE J-AGGREGATE OF A SQUARAIN		
DYE		30
3.1	Abstract	30
3.2	Introduction	30
3.3	Experimental Section	31
3.3.1	Preparation of the Spin-coated Films	31
3.3.2	Spectroscopic Measurements	32
3.4	Results and Discussion.....	32
3.5	Conclusion.....	38
APPENDIX A: ^1H AND ^{13}C NMR SPECTRA OF SQUARAIN DERIVATIVES		39
APPENDIX B: UV-VIS SPECTRAL DATA		42
APPENDIX C: PHOTOLUMINESCENCE SPECTRAL DATA.....		60
APPENDIX D: X-RAY DIFFRACTION DATA.....		62

APPENDIX E: NIR SPECTRAL DATA	67
LIST OF REFERENCES	71

LIST OF FIGURES

Figure 1-1: TGA thermograms of squaraine dyes. (a) SQC5(OH)2 exhibits decomposition temperature onset at 226 °C, (b) SQC5(OH)4n exhibits decomposition temperature onset at 283 °C, and (c) SQC5(OH)4b exhibits decomposition temperature onset at 281 °C.....	8
Figure 1-2: DSC thermograms of squaraine dyes. (a) SQC5(OH)2, (b) SQC5(OH)4n, and (c) SQC5(OH)4b.....	8
Figure 1-3: UV-vis absorption of squaraine dyes. (a) SQC5(OH)2, (b) SQC5(OH)4n, and (c) SQC5(OH)4b in CHCl ₃ solution.	9
Figure 1-4: Absorption and fluorescence emission of squaraine dye SQC5(OH)4 b in CHCl ₃ solution.	10
Figure 2-1: Schematic representation of H-and J-aggregates stacking as a result of π - π interaction. (a) H-aggregate (face-to-face), (b) J-aggregate (ladder-type), (c) J-aggregate (staircase-type), (d)J-aggregate (brickwork-type) ⁴⁵	14
Figure 2-2: Schematic representation of H-aggregate and J-aggregate spectral shifts according to the molecular exciton theory. ⁴⁹⁻⁵¹	16
Figure 2-3: SQC5(OH)2 absorption spectra: (a) spectrum of SQC5(OH)2 in chloroform dilute solution, (b) spectrum of the SQC5(OH)2 spin-coated thin film, (c) overlay liquid and solid state absorption spectra.	20
Figure 2-4: Effect of concentration (% w/w) on J-aggregates in spin coated thin film for squaraine dye SQC5(OH)2.	21

Figure 2-5: Absorption spectra of squaraine dyes series containing phenyl rings with two hydrox substituents and varying amino alkyl chain length.	22
Figure 2-6: UV-vis absorption spectra of SQC5(OH) ₄ n (a) spin-coated thin film, (c) dilute chloroform solution, and SQC5(OH) ₄ b (b) spin-coated film, (d) dilute chloroform solution.	24
Figure 2-7: UV-vis absorption spectra of spin-coated thin films of SQC6(OH) ₄ n, SQC10Ac(OH) ₄ n, SQC10Ac(OH) ₄ b, and SQC12(OH) ₄	25
Figure 2-8: UV-vis Absorption spectra of spin-coated thin films of SD3-4(OH) ₄ , and XL-SQ-3(OH) ₄	26
Figure 2-9: Photoluminescence spectra of SQC5(OH) ₂ (broad absorbance in black, sharp emission band in red).	27
Figure 2-10: X-ray diffraction patterns of squaraine dyes, SQC5(OH) ₂ , SQC5(OH) ₄ n, and SQC5(OH) ₄ b spin-coated thin films.....	28
Figure 3-1: UV-vis absorption of SQC5(OH) ₂ in chloroform solution. (b) UV-vis absorption of SQC5(OH) ₂ spin-coated thin film.	34
Figure 3-2: (a) The effect of temperature on optical absorption of a SQC5(OH) ₂ spin-coated film with increasing temperature. (b) Time dependent optical absorption of a SQC5(OH) ₂ spin-coated film at 60 °C.....	35
Figure 3-3: Plot of optical absorption of SQC5(OH) ₂ spin-coated film at 767 nm vs. time in seconds.	36
Figure 3-4: (a) Plot of ln k vs. 1/temperature (K x10 ⁻³). (b) Plot of ln k/T vs. 1/temperature....	37

LIST OF TABLES

Table 1-1: Thermal characteristics of squaraine dyes SQC5(OH) ₂ , SQC5(OH) _{4n} , and SQC5(OH) _{4b}	7
Table 1-2: Photophysical properties of squaraine dyes SQC5(OH) ₂ , SQC5(OH) _{4n} , and SQC5(OH) _{4b}	9
Table 3-1: Kinetics data of SQC5(OH) ₂ transformation	37

LIST OF SCHEMES

Scheme 1-1: The pathway procedure to synthesize the dihydroxy squaraine dye, 2,4-bis [4-(N,N-di-n-pentylamino)-2-hydroxyphenyl] squaraine, (SQC5OH) ₂	4
Scheme 1-2: The pathway procedure to synthesize the squaraine dyes with hydroxyl groups, 2,4-bis [4-(N,N-di-n-pentylamino)-2,6-dihydroxyphenyl] squaraine, (SQC5OH) ₄ n[R=C ₅ H ₁₁] 2,4-bis [4-(N,N-di-isopentylamino)-2,6-dihydroxyphenyl] squaraine and SQC5(OH) ₄ .b [R=C ₃ H ₅ (CH ₃)CH].....	5
Scheme 3-1: Chemical structure of squaraine dye derivative, SQC5(OH)₂ used to study the kinetics of J-aggregates	33

LIST OF ACRONYMS AND ABBREVIATIONS

^{13}C	Carbon-13 isotope
^1H	Hydrogen-1 isotope
2PA	Two-photon absorption
AFM	Atomic force microscopy
AU	Arbitrary unit
A- π -A	Aceptor- π -acceptor
ACN	Acetonitrile
CDCl_3	Deuterated chloroform
CF	Chloroform
CPS	Count per second
CT	Charge transfer
D	Doublet
DCE	Dichloroethane
dd	Doublet of doublets
D-A-D	Donor-acceptor-donor

DSC	Differential scanning calorimetry
EtOH	Ethanol
FTIR	Fourier transform infrared
g	Gram
GM	Gopper-Mayer unit for the 2PA cross section ($1 \times 10^{-50} \text{ cm}^4 \text{ s photon}^{-1} \text{ molecule}^{-1}$)
h	Hour
Hz	Hertz
<i>J</i>	Coupling constant
J	Joule
KHz	Kilohertz (10^3 Hertz)
KJ	Kilojoule (10^6 Joule)
L	Liter
LB	Langmuir Blodgett film
m	Multiplet
M	Molar

m.p.	Melting point
mg	milligram (10^{-3} gram)
MHz	Megahertz (10^6 Hertz)
μm	Micrometer 10^{-6} meter)
μL	Microliter (10^{-6} liter)
min	Minute
mL	Milliliter (10^{-3} Liter)
mmol	Millimole (10^{-3} mole)
mM	Millimolar (10^{-3} molar)
μM	Micromolar (10^{-6} molar)
ϵ	Molar absorptivity coefficient
MS	Mass spectrum
ms	Millisecond (10^{-3} second)
MW	Molecular weight
NIR	Near-infrared
nm	Nanometer (10^{-9} meter)

NMR	Nuclear magnetic resonance
PIC	Pseudo-isocyanine
PL	Photoluminescence
ppm	Parts per million
ppb	Part per billion
PV	Photovoltaics
r.t.	Room temperature
rpm	Revolution per minute
s	Second
S ₁	First excited state, singlet
S _n	Higher excited state
S ₀	Ground state, singlet
TFXRD	Thin film x-ray diffraction
TGA	Gravimetric analysis
THF	Tetrahydrofuran
TLC	Thin layer chromatography

UV	Ultraviolet
vis	Visible
W	Watt
λ_{\max}	Wavelength of maximum absorption
XRD	X-ray diffraction

CHAPTER 1: SQUARAIN DERIVATIVES SYNTHESIS AND CHARACTERIZATION

1.1 Abstract

Three squaraine dyes with different hydroxy groups attached to the dye and different alkyl chains were prepared and considered as models to investigate the aggregation behavior of each model. The thermal stability and behavior of the dyes were measured using differential scanning calorimetry (DSC) and thermogravimetric techniques. The photophysical properties of dilute solutions of the dyes were recorded using UV-vis and fluorescence spectroscopy to obtain values as baseline comparison for the investigation of the aggregation behavior in the thin film solid state.

1.2 Introduction

Squaraine compounds are an old class of chemicals. However, over the last few decades these types of dyes have been the subject of intensive studies due their unusual electronic properties that make them good candidates for a wide range of applications in various technological fields. They are particularly promising in nonlinear optics,¹ bioimaging for labeling and sensing of biomolecules,² sensitizers in solar cells and organic photovoltaics,³ two-photon absorbing materials, NIR-emitting fluorescent probes, second harmonic generation organic dyes, sensitizers for photodynamic therapy,⁴ and others.

Squaraine dyes tend to self-assemble or aggregate in useful molecular arrangements. The aggregates possess unique and useful properties that differ from the properties of the monomers. The most appealing characteristic is their absorption of light in the visible and infrared regions. The absorption is red-shifted or blue-shifted with respect to the monomer in solution, depending on the type of aggregation.

The aggregation of squaraine dyes derivatives in solution have been studied extensively.⁵⁻¹⁴ Only limited work and papers were published concerning the aggregation of squaraine derivatives in crystalline solid state thin films. The major part of those studies deals with Langmuir films.¹⁶⁻²⁰ Less work was done on spin-coated thin films produced from squaraine derivatives.²¹⁻²³

This research work presents the synthesis of series of squaraine derivatives with different alkyl substituents and numbers of hydroxyl groups. The monomers of these compounds were characterized and used to prepare spin-coated films. The solid state thin films were investigated using UV-vis spectroscopy and XRD (X-ray diffraction).

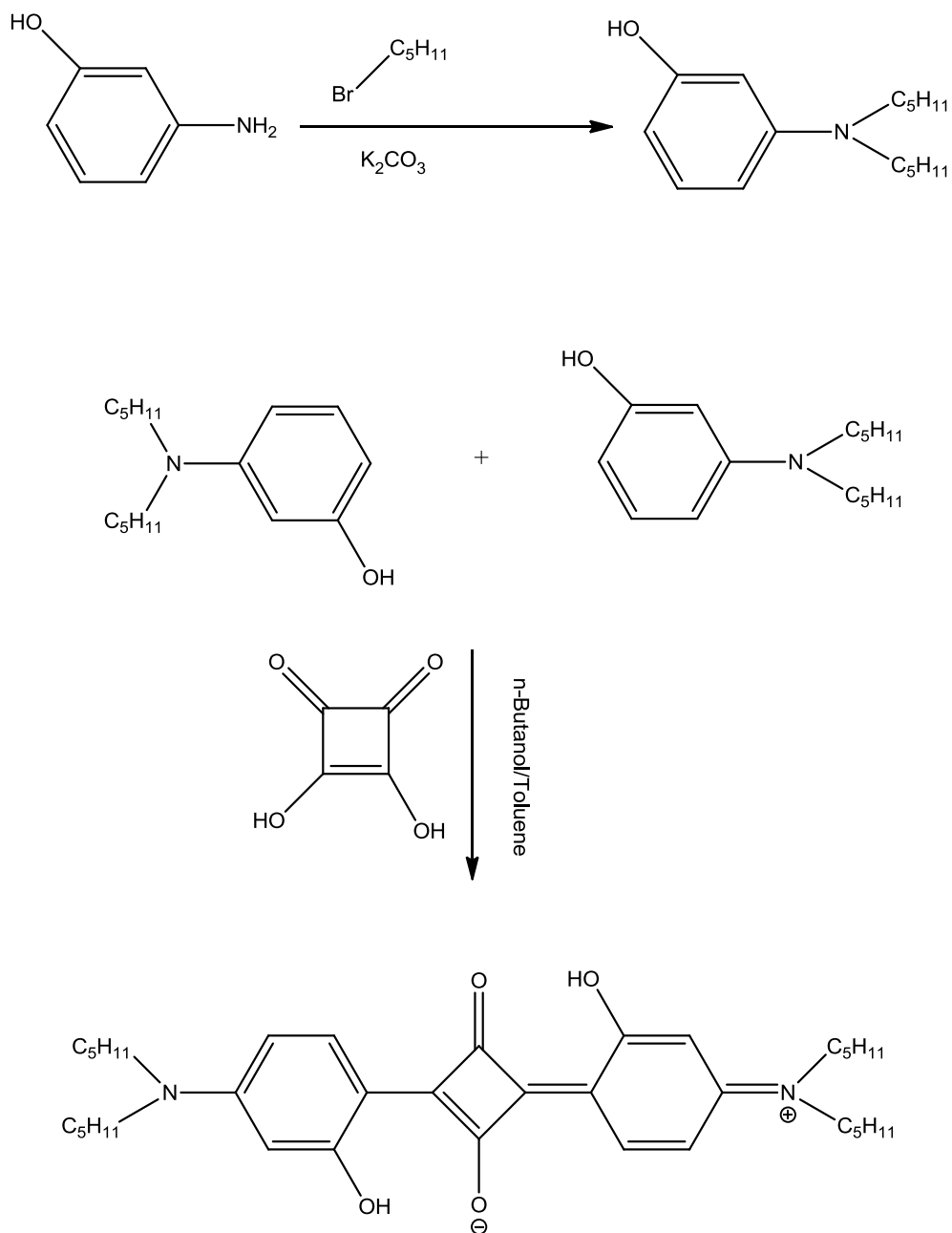
1.3 Experimental Section

1.3.1 Squaraine dyes preparation

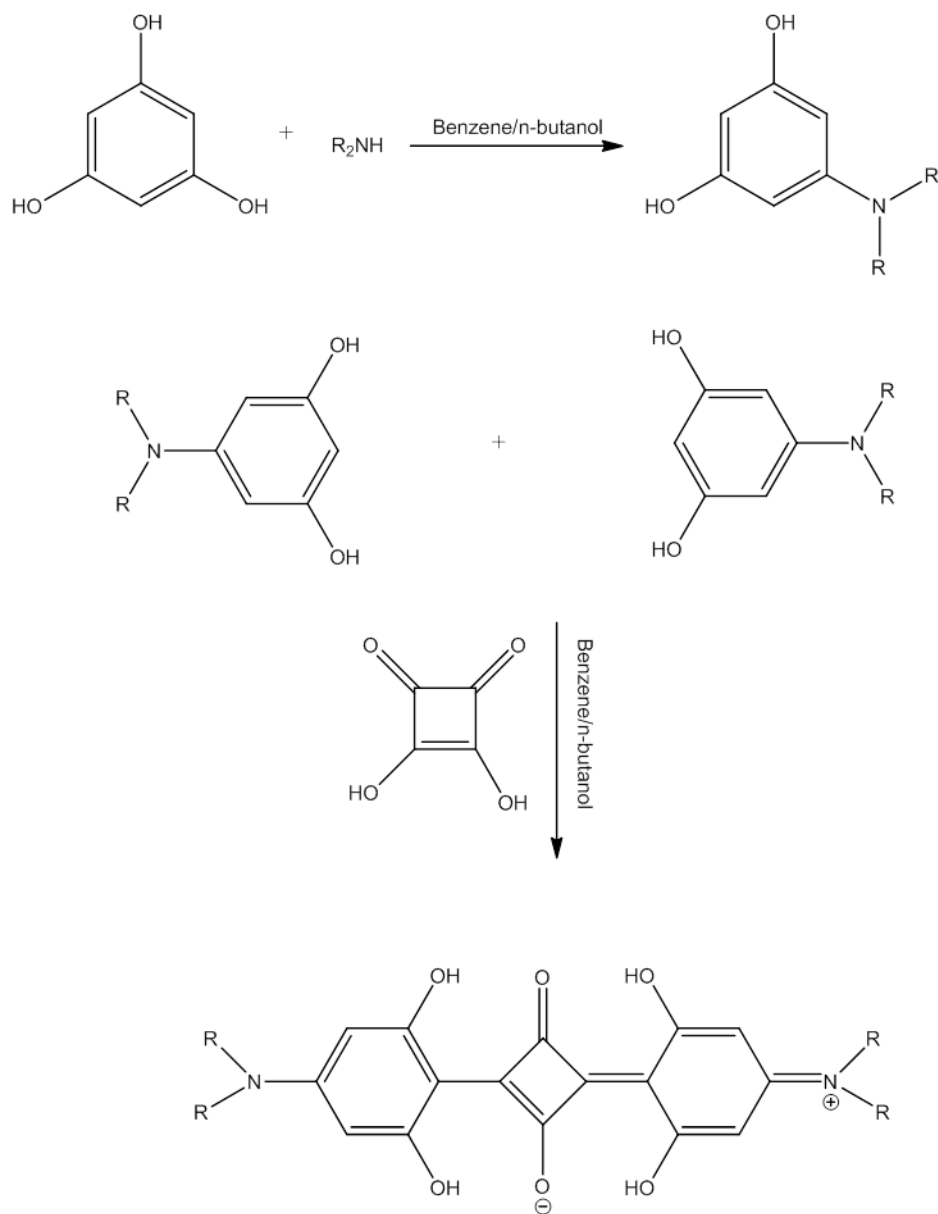
The preparation of symmetrical squaraine compounds was first reported by Sprenger *et al.*²⁴ This simple nucleophilic substitution reaction was widely used to prepare various versions of squaraine compounds.²⁵⁻²⁷ To synthesize symmetrical squaraine dyes with two hydroxy groups, two equivalents of an electron-rich aromatic compound were reacted with one equivalent of squaric acid (3,4-dihydroxycyclobut-3-ene-1,2-dione) in n-butanol/toluene. The mixture was

refluxed to obtain a good yield (higher than 50%)²⁵⁻²⁸ according to **Scheme 1.1**. Symmetrical squaraine compounds with four hydroxy groups attached to the phenyl ring are prepared by the same method using 1,3,5-trihydroxybenzene dihydrate as starting material but with lower yield^{25,29-30} as illustrated in **Scheme 1.2**.

Scheme 1-1: The pathway to synthesize the dihydroxy squaraine dye, 2,4-bis [4-(N,N-di-n-pentylamino)-2-hydroxyphenyl] squaraine, [SQC5(OH)2].



Scheme 1-2: The pathway to synthesize the squaraine dyes with four hydroxyl groups, 2,4-bis [4-(N,N-di-n-pentylamino)-2,6-dihydroxyphenyl] squaraine, (SQC5(OH)₄ n [R= C₅H₁₁] 2,4-bis [4-(N,N-di-isopentylamino)-2,6-dihydroxyphenyl] squaraine and SQC5(OH)₄.b [R=C₃H₅(CH₃)CH].



R= C₅H₁₁ for SQC5(OH)₄ n
C₃H₅(CH₃)CH for SQC5(OH)₄ b

1.3.2 Thermal Characterization

The decomposition temperatures of the squaraine dyes were recorded using a TGA Q5000 thermogravimetric analyzer (TA Instruments). The rate of heating was programmed at 10 °C/min from room temperature to 700 °C under a nitrogen atmosphere.

The transition temperatures of the dyes under study were measured using differential scanning calorimeter DSC Q1000 (TA Instruments). The heating rate was fixed at 10 °C/min for both the heating and cooling cycles. The sample and the reference were cooled to – 50 °C, heat up to 300 °C, then cooled back to -50 °C to investigate the thermal behavior of the squaraines during heating (melting) and cooling (crystalizing).

1.3.3 Photophysical Characterization

The steady-state absorption spectra of the squaraine dye solutions was recorded using an Agilent 8453 UV-vis spectrophotometer with a 10 mm path length quartz cuvette. The concentration of the squaraine dye solution was $\sim 1 \times 10^{-6}$ M in spectroscopic grade chloroform.

The steady-state photoluminescence (PL) measurements were obtained using a FLS 980 spectrofluorometer (Edinburgh Instruments). The concentration of the squaraine dye solution was $\sim 1 \times 10^{-6}$ M in spectroscopic grade chloroform.

^1H and ^{13}C NMR analyses were measured in CDCl_3 (referenced to TMS at δ 0.0 ppm) and recorded on Varian NMR spectrometers (500 or 300 MHz for ^1H and 75 MHz for ^{13}C).

1.4 Results and Discussion

The thermal stability study of squaraine dyes SQC5(OH)2, SQC5(OH)4 n, and SQC5(OH)4 b shows that the dyes with four hydroxyl groups were significantly thermally more stable and their decomposition temperatures were higher by more than 50 °C, as depicted in Table 1.1 and Figure 1.1.

Table 1-1: Thermal characteristics of squaraine dyes SQC5(OH)2, SQC5(OH)4n, and SQC5(OH)4b

	Decomposition	Phase Transition	Phase Transition	Melting Point	Melting Point
	Temperature, °C	Temperature, °C	Enthalpy, kJmol ⁻¹	Temperature, °C	Enthalpy, kJmol ⁻¹
SQC5(OH)2	226	NA	NA	185	47.5
SQC5(OH)4 n	283	2	3.76	226	22.4
SQC5(OH)4 b	281	NA	NA	NA	NA

The thermal behaviors of the squaraines were investigated by differential scanning calorimetry (DSC). The investigation shows that SQC5(OH)2 with two hydroxyl groups and di-n-pentyl chains, exhibited a very clear and sharp melting point at 185 °C while the SQC5(OH) with four hydroxyl groups and di- n-pentyl chains also showed a sharp melting point but at a higher temperature (226 °C) in addition to a transition at lower temperature (2 °C). The squaraine with

branched alkyl chains, SQC5(OH)4b did not show any melting point nor any other thermal transition such as recrystallization. It decomposed at 281 °C without any phase transition as illustrated in Figure 1.2 and Table 1.1. This phenomenon and recrystallization can be ascribed to the branched chains which make the dye less flexible and hinder the packing and consequently the recrystallization of the material after heating.

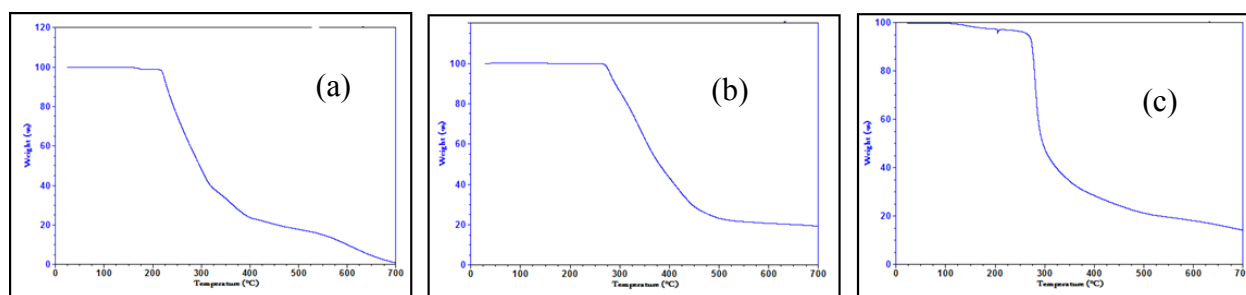


Figure 1-1: TGA thermograms of squaraine dyes. (a) SQC5(OH)2 exhibits decomposition temperature onset at 226 °C, (b) SQC5(OH)4n exhibits decomposition temperature onset at 283 °C, and (c) SQC5(OH)4b exhibits decomposition temperature onset at 281 °C.

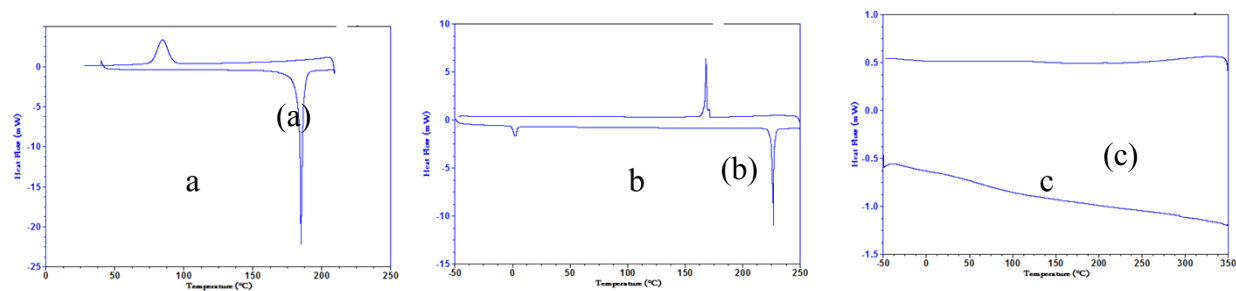


Figure 1-2: DSC thermograms of squaraine dyes. (a) SQC5(OH)2, (b) SQC5(OH)4n, and (c) SQC5(OH)4b.

The UV-vis absorption spectra (Figure 1.3) indicate very little difference in λ_{max} for the three dyes. However, the shoulder that appears before the maximum absorption band is more obvious for the squaraine dyes with four hydroxy groups. The dyes are all fluorescent in dilute solution with a small Stokes shift. (Table 1.2 and Figure 1.4)

Table 1-2: Photophysical properties of squaraine dyes SQC5(OH)2, SQC5(OH)4n, and SQC5(OH)4b.

	Molar Absorptivity, ϵ	Absorption λ_{max}	Emission λ_{max}	Stock shift
	$\text{Lmol}^{-1} \text{ cm}^{-1}$	nm	nm	nm
SQC5(OH)2	1.9×10^5	645	661	16
SQC5(OH)4 n	2.2×10^5	649	664	15
SQC5(OH)4 b	2.0×10^5	649	665	16

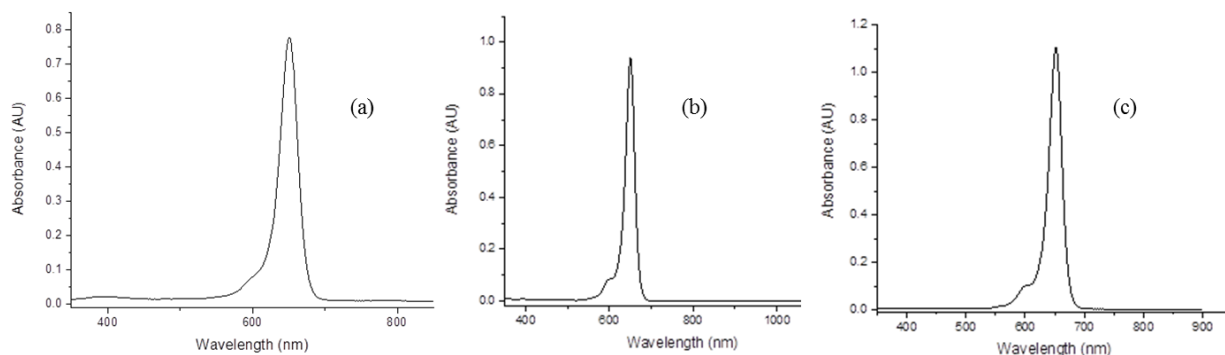


Figure 1-3: UV-vis absorption of squaraine dyes. (a) SQC5(OH)2, (b) SQC5(OH)4n, and (c) SQC5(OH)4b in CHCl_3 solution.

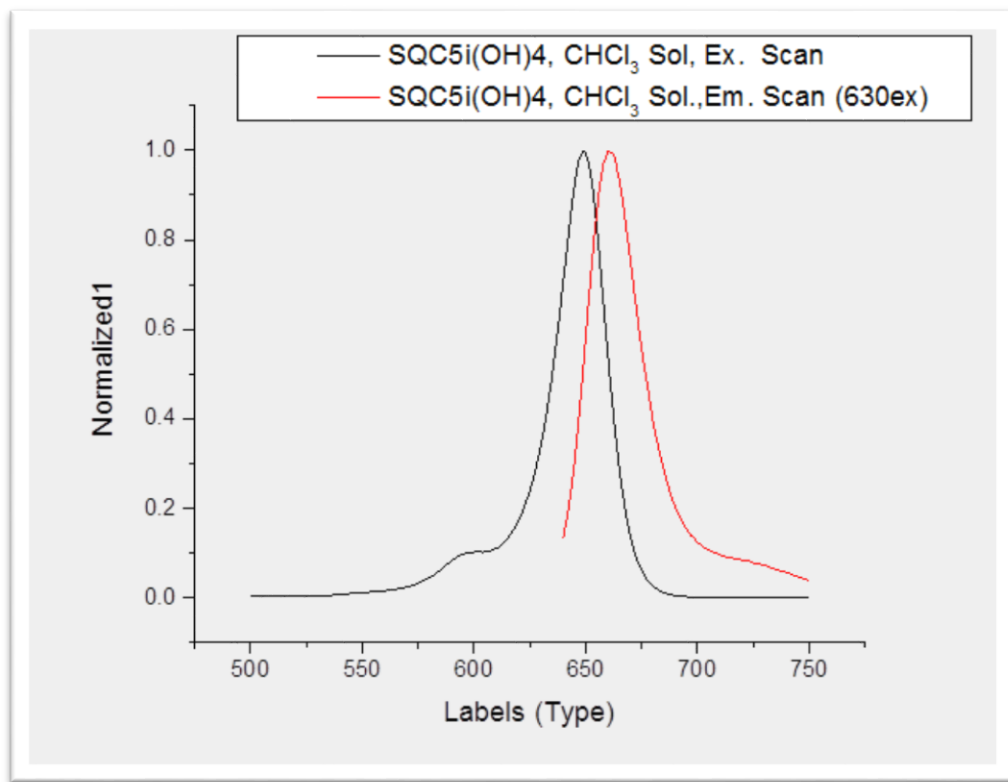


Figure 1-4: Absorption and fluorescence emission of squaraine dye SQC5(OH)4 b in CHCl₃ solution.

1.5 Conclusion

The number of hydroxy groups attached to the squaraine compounds exerts a significant effect on the thermal properties of the dye. Squaraine dye derivatives with four hydroxy groups possess higher thermal stability and higher melting point, which may be ascribed to the fact that dyes with four hydroxy groups can form more hydrogen bonds compared to those with only two hydroxy groups, resulting in a more planar, rigid, and stabilized squaraine core. The branched version of SQC5(OH)₄ b did not exhibit a melting point but, like the normal chain analog, it decomposed at higher temperature. The photophysical properties of these dyes in dilute solution were similar.

CHAPTER 2: INVESTIGATION OF SQUARINE DERIVATIVES AGGREGATION IN SOLID STATE SPIN-COATED THIN FILMS

2.1 Abstract

The squaraine dyes, 2,4-bis [4-(N,N-di-n-pentylamino)-2-hydroxyphenyl] squaraine [SQC5(OH)2], 2,4-bis [4-(N,N-di-n-pentylamino)-2,4-hydroxyphenyl] squaraine [SQC5(OH)4 n], and 2,4-bis [4-(N,N-di-isopentylamino)-2,4-hydroxyphenyl] squaraine [SQC5(OH)4 b] were investigated to study their aggregation in solid state thin film form using UV-vis absorption spectroscopy technique. The investigation revealed significant difference in aggregation behaviors and features. The dye SQC5(OH)2 mainly exhibits J-type aggregation with intense absorption band near infrared region. In contrast, the SQC5(OH)4 n and SQC5(OH)4 b compounds mainly exhibit H-type aggregation characterized by less intense and blue-shifted absorption bands. The resulting broad absorption of the squaraine solid state films should be amenable to broad band visible and NIR light energy harvesting.

2.2 Introduction

Since its first discovery, independently, by Jelly³¹ and Scheibe³² in 1930s, J-aggregates of chemical dyes have the subject of intense and continuous work by chemists and material scientists due to the fact that these materials possess unique properties. As a matter of fact they open a large window for promising applications in a wide spectrum of technological fields.

Jelly and Scheibe noticed the formation of a new absorption band in concentrated solution of pseudo-isocyanine (PIC) dye.^{31,32} This band is red shifted (bathochromic shift) in respect to the monomer in solutions. It is characterized as narrow with a very high absorption coefficient (ϵ) and strong fluorescence with small Stokes shift. Another type of aggregate is blue shifted (hypsochromic shifted) and referred to as H-aggregates. Unlike J-aggregates, H-aggregates do not exhibit any fluorescence.^{33,34}

After the observation of the aggregation phenomenon of dyes, the major focus was on studying the aggregation of cyanine dyes. A tremendous number of studies were published about property-structures relationships of those dyes and their potential applications in various technical fields.

The work was extended to include other types of chemical dyes such as merocyanine and squaraine dyes. The last dyes are a class of dyes that, in contrast to cyanine dyes, are nonionic and are excellent candidates for a large number of applications such as imaging, nonlinear optics, and particularly in photovoltaics.^{3, 42-44}

Both H-and J-aggregates have strong absorption bands in the visible and NIR regions, respectively. This change in absorption of the H- and J-aggregates with respect to the monomer in dilute solution indicates that the self-assembled molecules have significantly different electronic structures than the monomer. This difference can be ascribed to the large transition moment parallel to the long axis of the chromophore. Huhn and coworkers⁴⁵ proposed a model to represent the arrangement of molecules (dipoles) in H- and J- aggregates as illustrated in Figure 2.1.

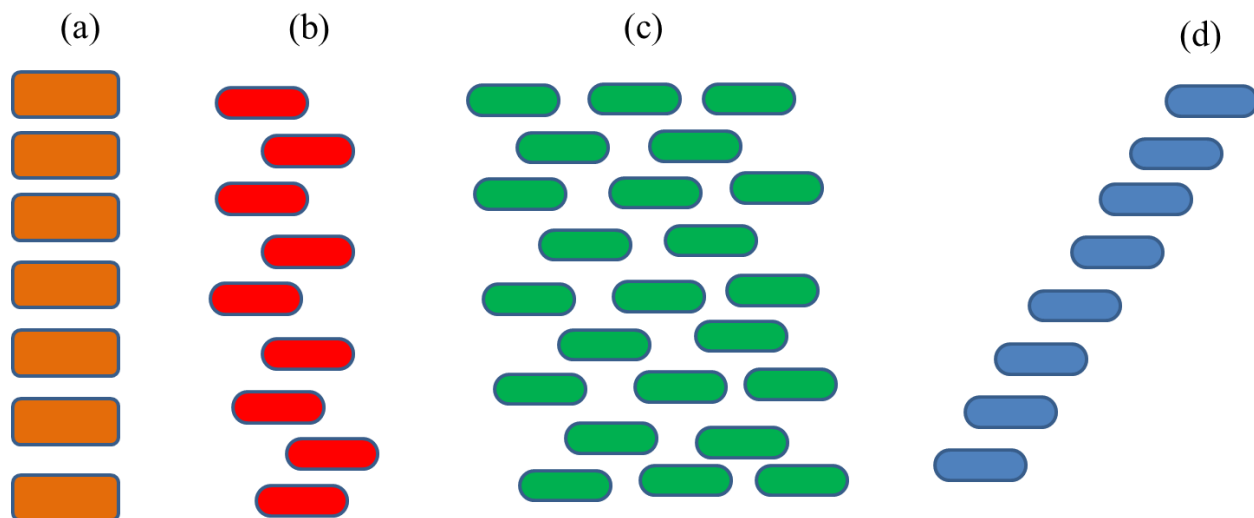


Figure 2-1: Schematic representation of H- and J-aggregates stacking as a result of π - π interaction. (a) H-aggregate (face-to-face), (b) J-aggregate (ladder-type), (c) J-aggregate (staircase-type), (d) J-aggregate (brickwork-type)⁴⁵.

The H-aggregates have a face-to-face arrangement while in the J-aggregates the molecules are arranged end-to-end (head-to-tail). In J-aggregates, the molecules can stack in three manners: ladder, staircase, or brickwork.⁴⁵

The shift in the absorption band for both H- and J-aggregates with respect to the monomer can be explained using the molecular exciton theory. Based on this theory the dye molecules are considered as dipole points. When two transition dipoles interact, the excitonic state of the dye molecules splits into two energy states as shown in Figure 2.2. If the dipoles are arranged in face-to-face model and parallel (H-aggregate), the dipoles repel each other leading to a high energy (S_2 in Figure 2.2) while in the antiparallel case, the dipoles attract each other resulting in a lower energy state (S_1). It has been reported that for parallel transition dipoles, the transition from S_0

(ground state) to S_1 (excited state) is forbidden; by contrast, the transition from S_0 to S_2 is allowed.⁴⁸ In the H-aggregate arrangement, the angle between the long axis of the dye molecule and the straight line is significantly larger.⁴⁷⁻⁴⁹

In J-aggregates the two dipoles are end-to-end (head-to-tail) arranged. The synchronous dipoles get the lower energy (S_0 to S_1) while the reverse dipoles have the highest energy (S_0 to S_2). For this arrangement only the transition from S_0 (ground state) to S_1 is allowed and the angle between the long axis of the dye molecule and the straight line is smaller with respect to the face-to-face arrangement (H-aggregate).⁴⁹⁻⁵¹

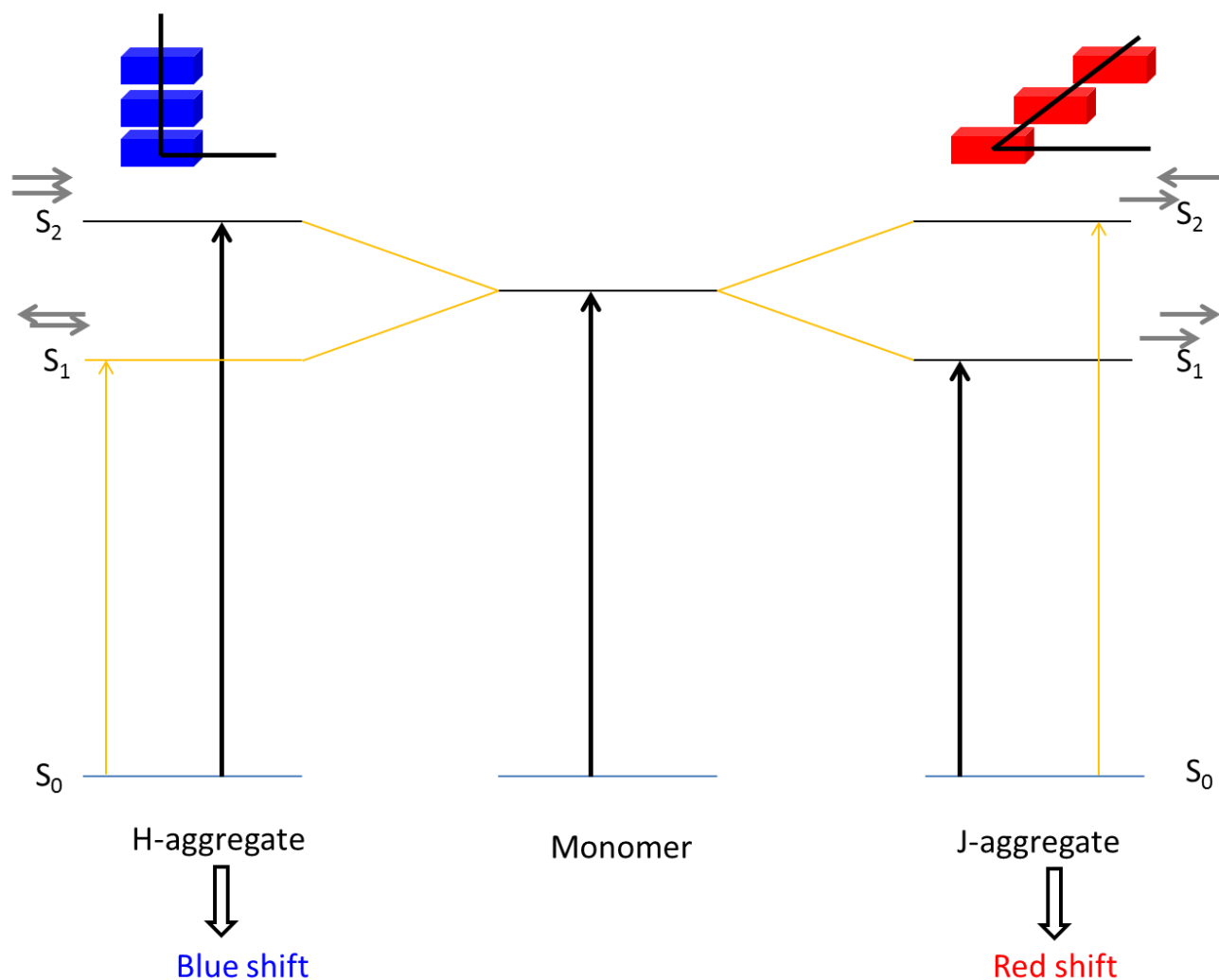


Figure 2-2: Schematic representation of H-aggregate and J-aggregate spectral shifts according to the molecular exciton theory.⁴⁹⁻⁵¹

In the last few decades, organic photovoltaic (OPV) cells have become the subject of intense research due to their great potential as renewable energy sources. Despite their low power conversion efficiency, which have been improved approaching 8%⁷¹, OPV possess a high

completion edge over conventional solar cells materials because to their unique features such as low-cost of manufacturing, light weight, facile to synthesis and flexibly.⁷²⁻⁷⁴

Squaraine dyes have demonstrated high potential to be used as donor materials in solar cell technology because of their high absorption coefficient and intense and broad absorption in the visible and NIR spectral regions. The J-aggregate of squaraine derivatives in solid state thin film is attracting more researches in the field of solar cells due the spectral match of the absorption of the film with solar spectrum which is an important factor in the efficient light conversion.⁷³

2.3 Experimental Section

2.3.1 Spectroscopic Measurements

UV-vis measurements of the spin-coated thin films were recorded using an Agilent 8453 spectrophotometer (Agilent Technologies). A solid state holder was constructed to accommodate the spin-coated thin film samples. The holder is equipped with heating elements and a temperature control device to allow the measurement of the absorption at different temperatures.

2.3.2 Preparation of the Spin-coated Films

The squaraine compound **SQC5(OH)2** was dissolved in spectroscopic grade chloroform (Aldrich) to obtain 1% w/w solution. This solution was used to fabricate spin-coated thin films. The solution was spread out on previously precleaned and solvent cleaned quartz substrates. A spin-coating system (G3P SPINCOAT, from Cookson Electric Equipment) at 3000 rpm was used

to obtain the thin films. The spin-coating parameters were optimized in order to produce roughly homogenous thickness thin films of approximately 100 nm. The squaraine spin-coated substrates were vacuum dried for several hours to remove residual solvent prior to performing UV-vis spectroscopic and other measurements.

2.3.3 Photoluminescence Measurements

Photoluminescence (PL) measurements of the spin-coated thin films were obtained using FLS 980 spectrofluorometer (Edinburgh Instruments) equipped with a special holder for solid state measurements.

2.3.4 Thin Film X-ray Diffraction Measurements

X-ray diffraction pattern of the thin films of the squaraine dyes were collected from MiniFlex diffractometer (SamrtLab, Ragu Co.) using continuous scan mode and 4.000 deg/min scan speed.

2.4 Results and Discussion

Squaraine derivatives are known in literature to absorb light in the visible region between 625 and 665 nm, depending on the substituents at the nitrogen atom and the substituents in the phenyl groups.^{52,53} As a result of the strong intermolecular charge-transfer interactions, the absorption spectral band is red shifted (bathochromic shift) or blue shifted (hypsochromic shift) in thin film solid state forms.

To explore and investigate J- and H-aggregate formation in squaraine compounds, several squaraine dyes were studied. The symmetrical dye, 2,4-bis[4-(N,N)-di-n-pentylamino)-2-hydroxyphenyl] squaraine, SQC5(OH)₂ was used as a model for squaraine dyes derivatives with two hydroxy substituents in the phenyl ring. UV-vis spectroscopic measurements performed on thin films of approximately 100 nm thick revealed the presence of a sharp and intense band at 767 nm with a shift in wavelength of 117 nm compared to the absorption band of the monomeric form in dilute solution (650 nm) as seen in Figure 2.3.

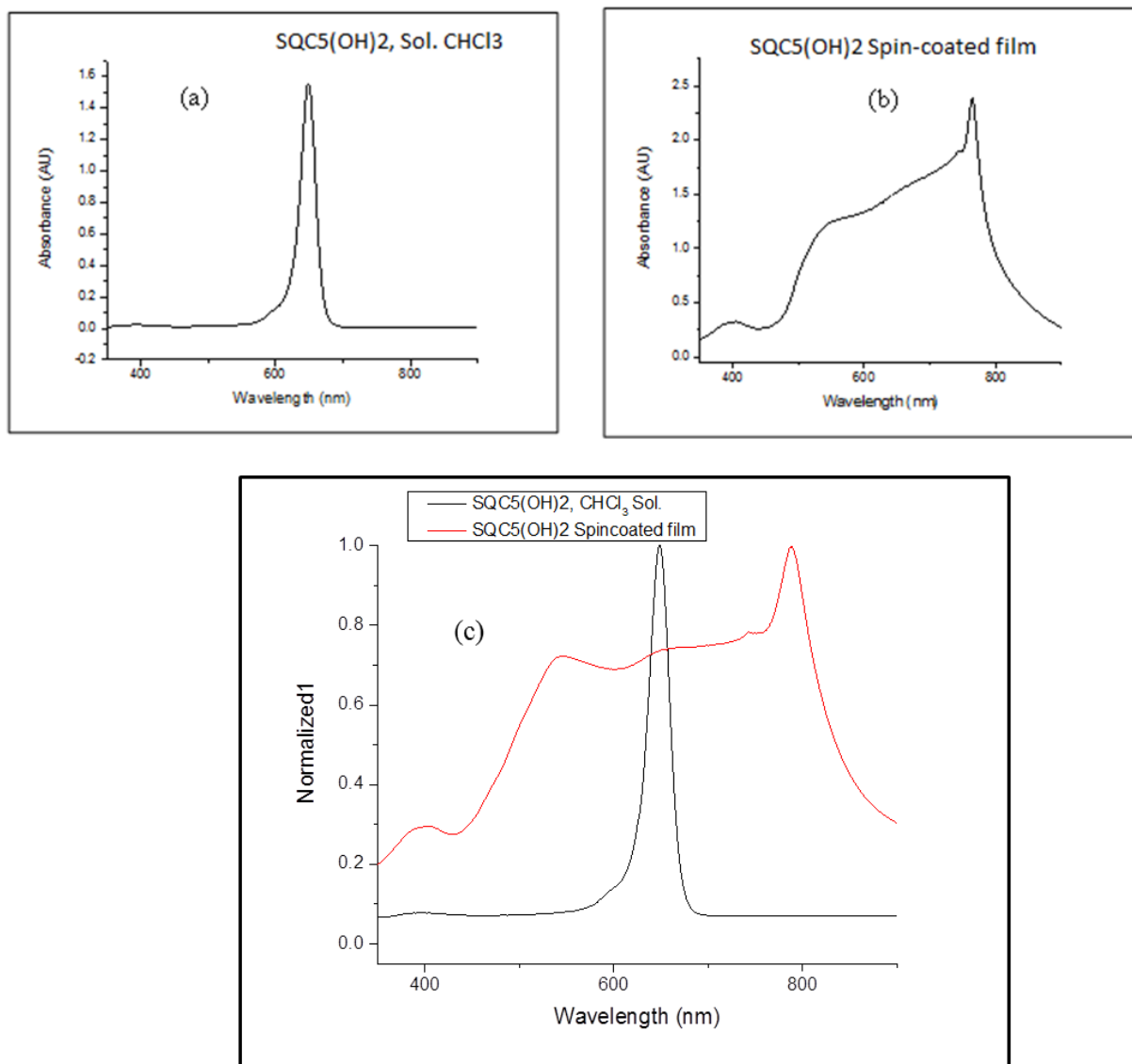


Figure 2-3: SQC5(OH)2 absorption spectra: (a) spectrum of SQC5(OH)2 in chloroform dilute solution, (b) spectrum of the SQC5(OH)2 spin-coated thin film, (c) overlay liquid and solid state absorption spectra.

This red shifted band was observed for thin films obtained by spin-coating on quartz substrates using 1% w/w solution. Its red shift depends to some extent on the solution concentration, as can be seen in Figure 2.4.

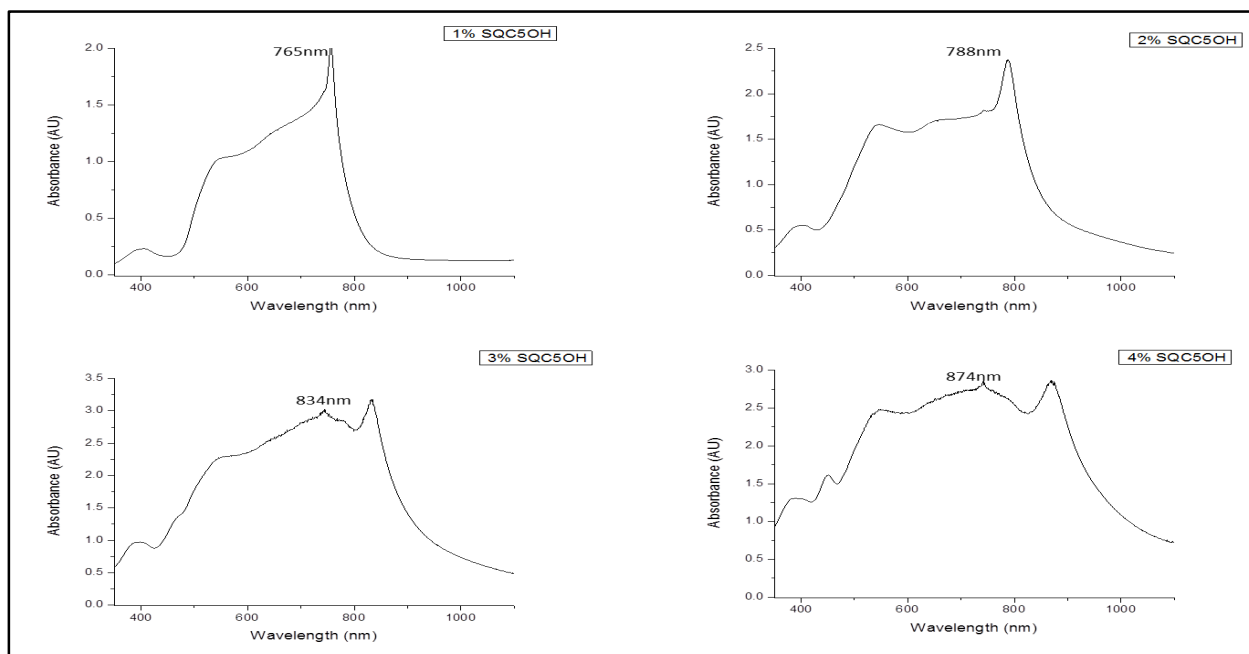


Figure 2-4: Effect of concentration (% w/w) on J-aggregates in spin coated thin film for squaraine dye SQC5(OH)₂.

Figure 2.5 shows the spectral absorption of other squaraine dye derivatives studied in this work. All of them showed less red shift relative to SQC5(OH)₂ with broader bands. These data reveal that the N-alkyl substituents have a significant effect on the aggregation of the dyes in the solid state thin film.

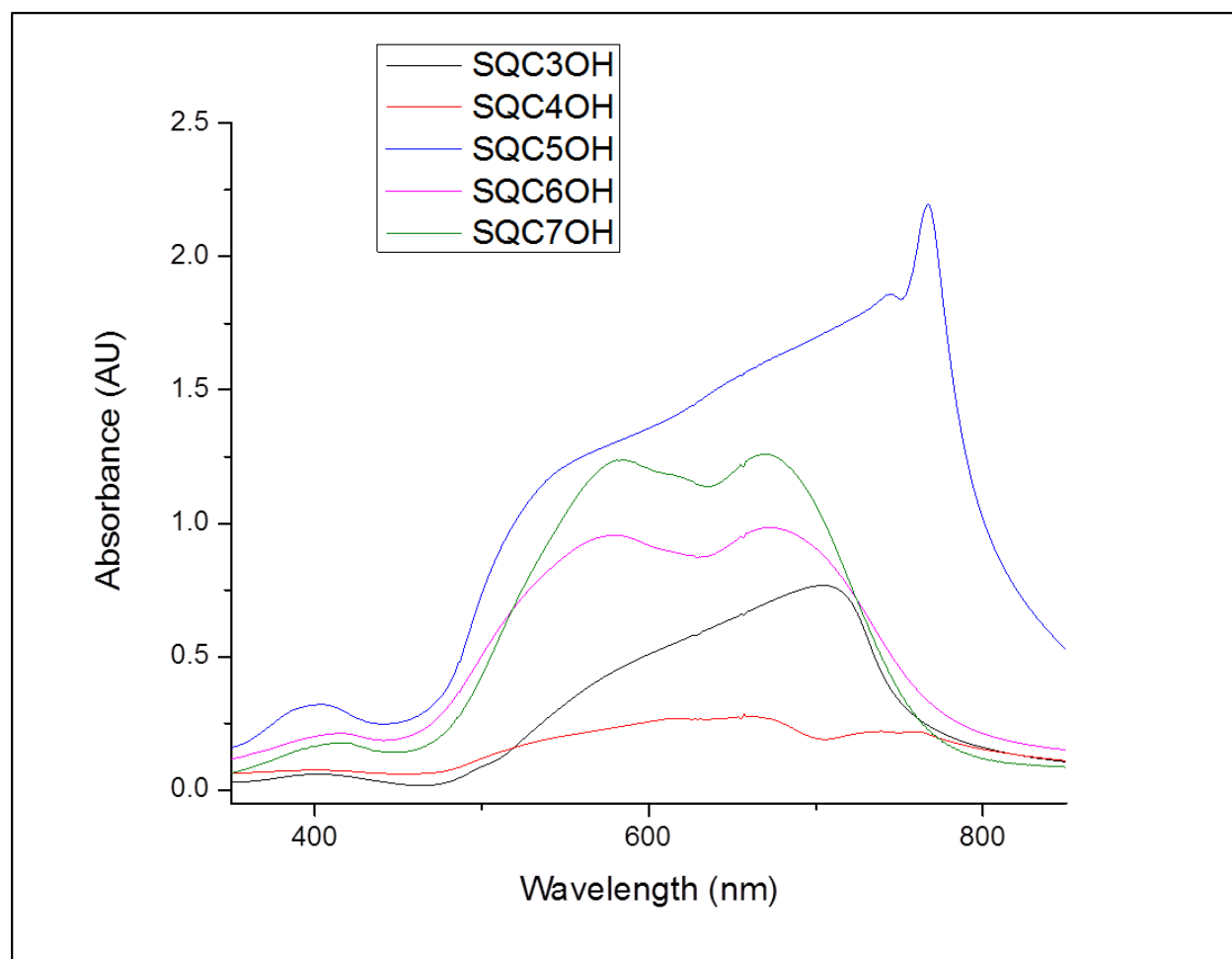


Figure 2-5: Absorption spectra of squaraine dyes series containing phenyl rings with two hydrox substituents and varying amino alkyl chain length.

In contrast to the symmetrical squaraine dye, SQC5(OH)₂, containing two hydroxyl groups attached to phenyl rings, spin-coated thin films of symmetrical squaraine dyes with four hydroxyl groups have blue shift absorption bands with respect to the monomer in liquid solution. Figure 2.6

The dye 2,4-bis[4-(*N,N*-dipentylamino)-2,6-dihydroxyphenyl] squaraine, SQC5(OH)₄ n, reveals the formation of a sharp and intense absorption band with λ_{max} at 560 nm, which is blue shifted by 90 nm with respect to the absorption band of the monomer in liquid solution. It also exhibited a red shifted smaller absorption band at approximately 660 nm (~10 nm red shift). The absorption band at 560 nm can be attributed to the formation of face-to-face arrangement to result in H-aggregation when the squaraine compound was spin-coated from the solution. While the smaller red shifted absorption band with λ_{max} at 660 nm can be explained by the formation of a small amount of the J-aggregate or possibly due to the slight red-shift of the monomer absorption in solid state.

Unlike the n-pentyl version of the symmetrical squaraine dye, SQC5(OH)₄ n, 2,4-bis[4-(*N,N*-isodipentylamino)-2,6-dihydroxyphenyl] squaraine, SQC5(OH)₄ b, showed a broader absorption band at 620 nm (20 nm blue shift) with a shoulder at approximately the same absorption as the absorption of the monomer in liquid solution, as depicted in Figure 2.6.

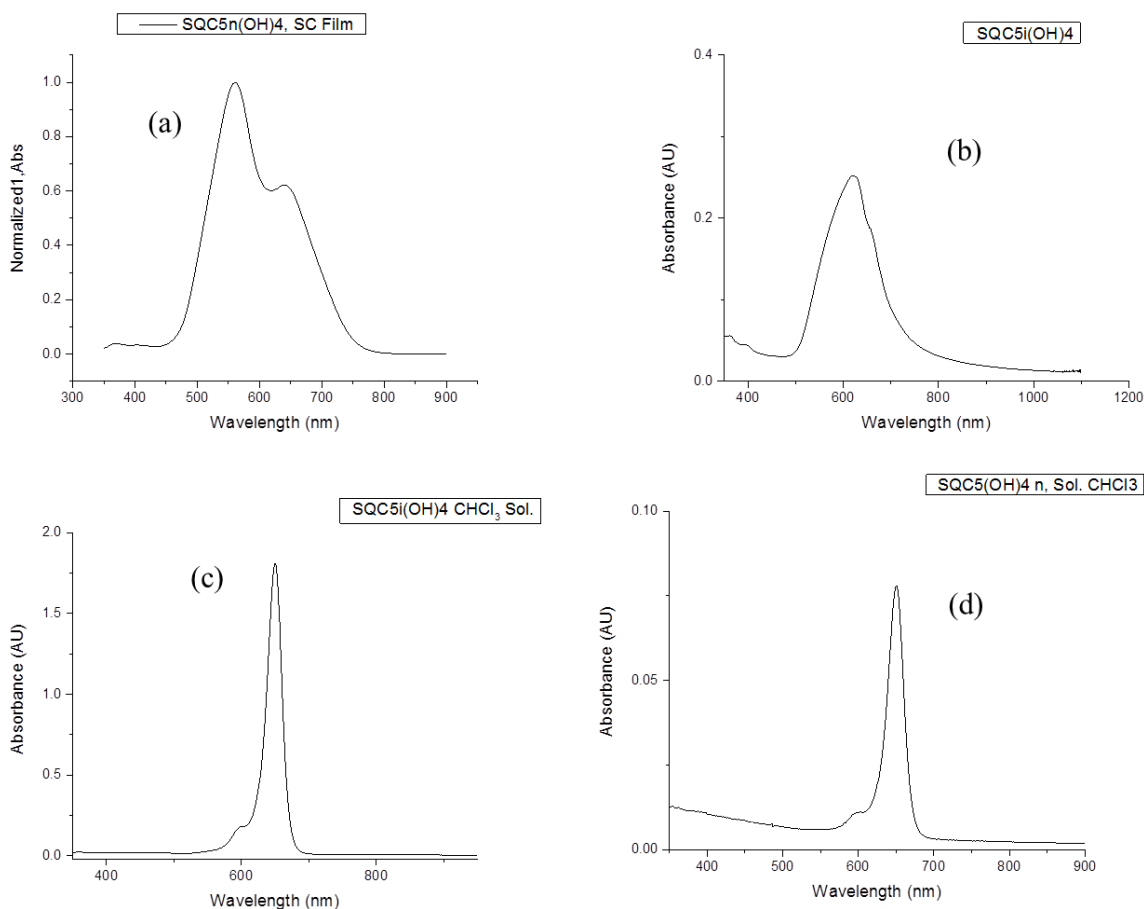


Figure 2-6: UV-vis absorption spectra of SQC5(OH)4 n (a) spin-coated thin film, (c) dilute chloroform solution, and SQC5(OH)4 b (b) spin-coated film, (d) dilute chloroform solution.

To confirm the observation that squaraine dye derivatives possessing two hydroxyl substituents at the phenyl form mainly J-aggregates with head-to-tail molecular arrangement, while the squaraine derivatives with four hydroxy groups form mainly blue shifted face-to-face H-aggregates, other squaraine dyes derivatives, SQC6(OH)4n, SQC10Ac(OH)4n, SQC10Ac(OH)4b, SQC12(OH)4, SD3-4(OH)4, and XL-SQ-3(OH)4, with different donor N-substituents and the same number of hydroxy substituents (four) were explored. They all exhibited the formation of H-aggregates as illustrated in Figures 2.7 and 2.8.

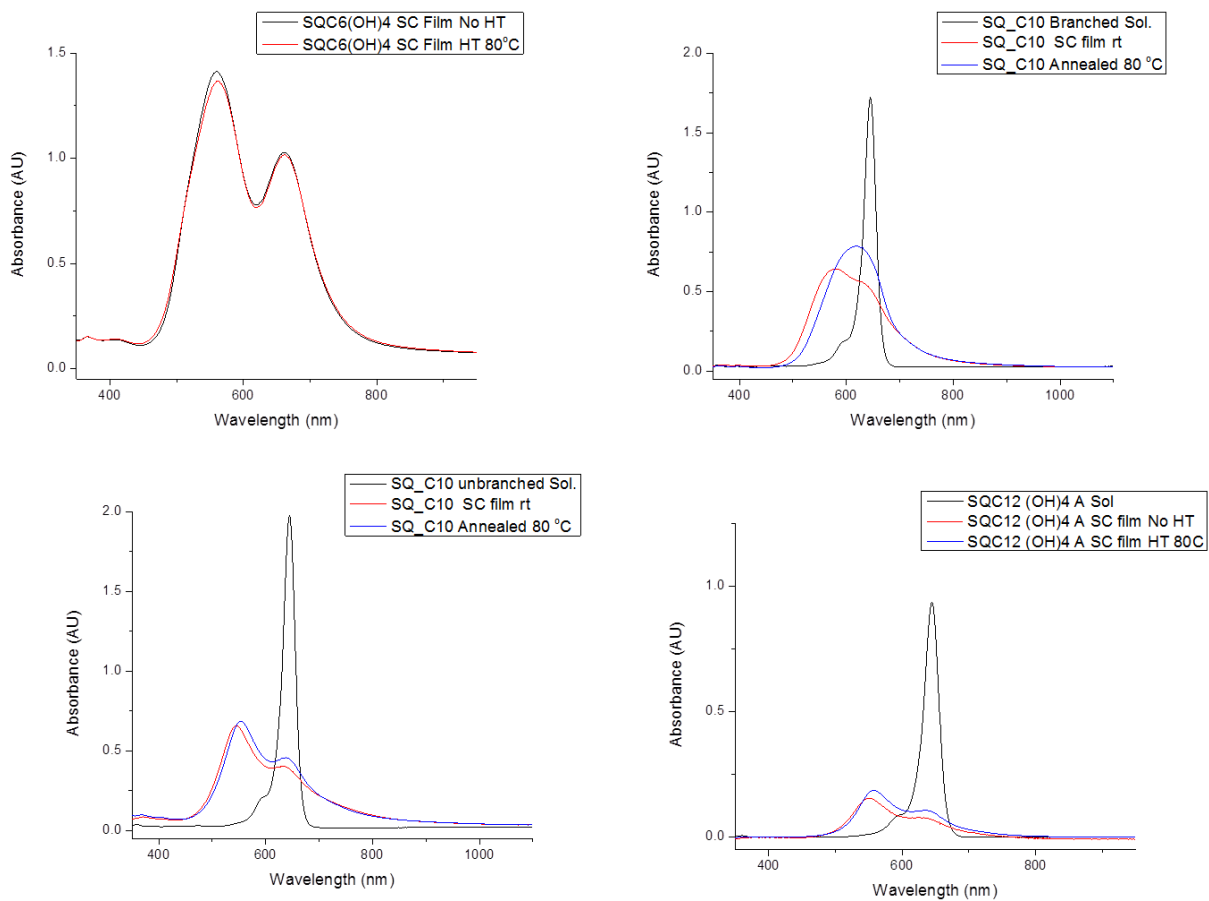


Figure 2-7: UV-vis absorption spectra of spin-coated thin films of SQC6(OH)4 n, SQC10Ac(OH)4 n, SQC10Ac(OH)4 b, and SQC12(OH)4.

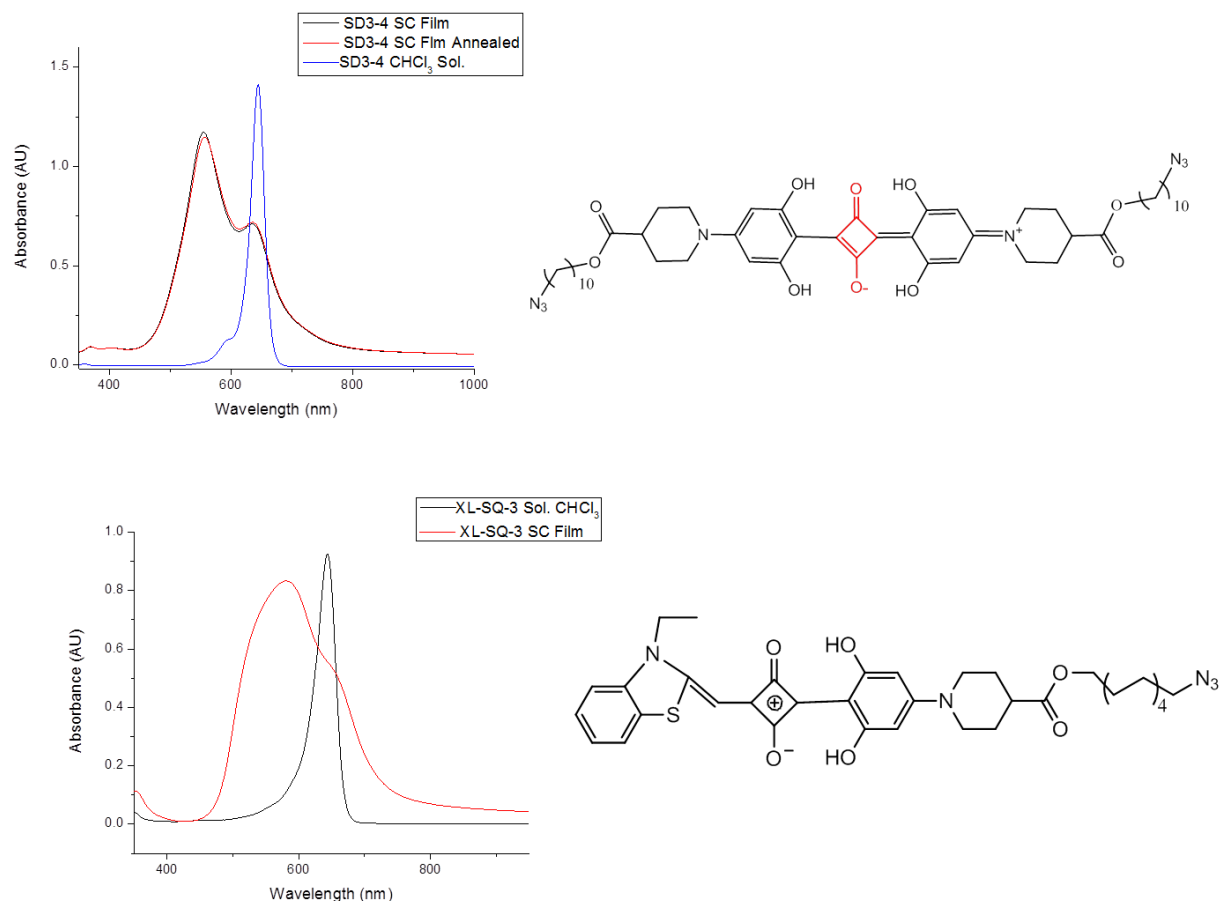


Figure 2-8: UV-vis Absorption spectra of spin-coated thin films of SD3-4(OH)₄, and XL-SQ-3(OH)₄

The above phenomenon of squaraine dye derivatives containing hydroxy substituents that form primarily H-aggregates may be explained by the stronger hydrogen bonding which promotes the face-to-face arrangement of molecules instead of end-to-end arrangement through making the central squaraine core more rigid and planar, promoting face-to-face intermolecular interactions.

To further investigate the bathochromic and hypsochromic shifts of the squaraine dye derivatives in thin spin-coated films, photoluminescence properties were evaluated. SQC5(OH)₂

was excited at 660 nm, resulting in a narrow emission band with a maximum at 771 nm and a very small Stokes shift (4 nm), as can be seen in Figure 2.9. The thin films spin-coated using SQC5(OH)4 n and SQC5(OH)4 b exhibited no photoluminescence emission a feature that is consistent with H-aggregation^{30,34}.

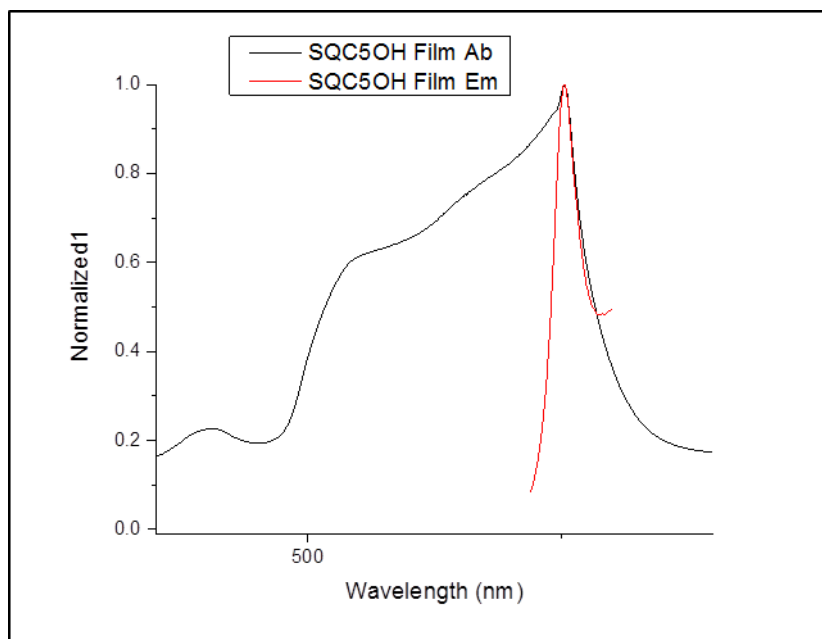


Figure 2-9: Photoluminescence spectra of SQC5(OH)2 (broad absorbance in black, sharp emission band in red).

Thin film X-ray diffraction measurements were carried out for spin-coated films of SQC5(OH)2, SQC5(OH)4 n, and SQC5(OH)4 b to further investigate the difference between the bathochromic shifted J-band and the hypsochromic shifted H-band⁵⁴. The XRD scans (2θ scans) of the thin films show that SQC5(OH)2 has very intense peak at 4.9 while in SQC5(OH)4 n and

SQC5(OH)4 b, very low intensity signals were observed at 5.3 and 7.5, respectively as shown in Figure 2.10.

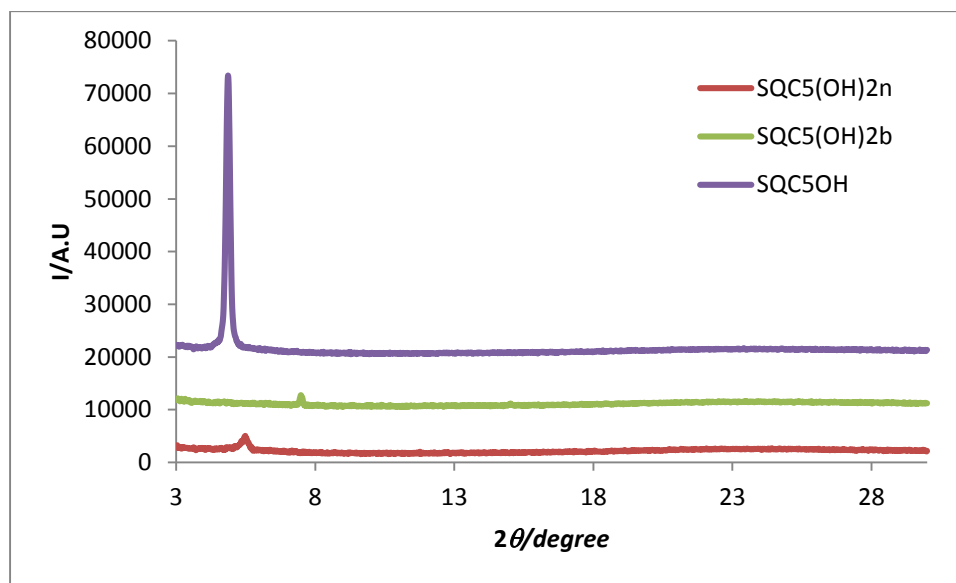


Figure 2-10: X-ray diffraction patterns of squaraine dyes, SQC5(OH)2, SQC5(OH)4 n, and SQC5(OH)4 b spin-coated thin films.

2.5 Conclusion

Squaraine dye derivatives containing two hydroxy groups in their phenyl ring aggregate when spin-coated from a chloroform solution in J-type aggregation. The observed J-absorption band was significantly red shifted with respect to the absorption band of the monomeric form of the dye in liquid solution. This band is characterized by an intense absorption, characteristic of J-aggregation. By contrast, the squaraine dye derivatives with four hydroxy groups form H-type

aggregates. The H-absorption band was blue shifted and broader than the absorption band of the monomer in solution.

The photoluminescence study on the solid state thin films of the squaraine dyes reveals that the squaraine compound with two hydroxy groups was florescent with a small Stokes shift while the squaraine dyes with four hydroxy substituents on the phenyl rings adjacent to the squaraine core exhibited no photoluminescence. These observations are consistent with formation of J- and H-aggregates, respectively. The thin film X-ray diffraction (TFXRD) scans of the three squaraine derivatives, SQC5(OH)₂, SQC5(OH)₄ n, and SQC5(OH)₄ b, exhibited significantly different patterns indicating different packing patterns and crystalline structures.

The resulting broad absorption of the squaraine solid state films should be of interest to those working in the organic dye-sensitized solar cells field for broad band visible and NIR electromagnetic radiation energy harvesting.

CHAPTER 3: KINETIC INVESTIGATION OF THE J-AGGREGATE OF A SQUARINE DYE

3.1 Abstract

The aggregation behavior of the squaraine dye derivative 2,4-bis [4-(N,N-di-n-pentylamino)-2-hydroxyphenyl] squaraine [**SQC5(OH)2**] in solid state spin-coated thin films was investigated. The study reveals the formation of J-aggregates with bands at 767 nm at room temperature. This aggregate was temperature dependent; it decayed with increased temperature. The activation energy of the decay process was found to be 91.2 kJ. The values of ΔH and ΔS are 88.4 kJ/mol and 48.2 J/K.mol, respectively.

3.2 Introduction

Squaraine dyes have gained a tremendous attention due to their wide spectrum of applications such as optical devices,^{55,56} solar cells⁵⁷ and nonlinear optics.⁵⁸ In liquid solutions; these dyes form J-aggregates that are characterized by a sharp absorption in the visible or NIR region.⁵⁹ The formation of J-aggregate is effected by several factors.^{60,61} The solid state J-aggregate shows a broader band due to the intermolecular charge-transfer interactions.⁵⁵ Hydroxy groups on the phenyl rings adjacent to the squaraine core effect both the formation of H-and J-aggregation of Langmuir films.⁶² Squaraine dyes without hydroxyl groups were found the form J-aggregates in Langmuir films.⁶³ Heat-treatment and treatment with acetic acid vapor red shifts the J-band of the spin-coated thin films and improves its sharpness J-band.⁶⁴ A squaraine dye with two hydroxyl

groups was selected to functionalize carbon nanotubes. The J-aggregates effectively photosensitize carbon nanotubes.⁶⁵ Squaraine dye derivatives possess a high third-order nonlinear optical coefficient, $\chi^{(3)}$. This feature, in addition to their good processability, ability to form large-area films, and comparatively low cost, provides them with high competitive factors in optical devices applications⁶⁶. Optically active J-aggregates can be described by a sigmoidal time dependence.⁶⁷ The formation of J-aggregates on the surface of Au colloidal dispersion was reported to occur through two-steps mechanism.⁶⁸ Understanding the solid state behavior of squaraine aggregation and factors that may be harnessed to modulate it are of growing interest.

3.3 Experimental Section

3.3.1 Preparation of the Spin-coated Films

The squaraine compound **SQC5(OH)2** was dissolved in spectroscopic grade chloroform (Aldrich) to obtain 1% w/w solution. This solution was used to fabricate spin-coated thin films. The solution was spread out on previously precleaned and solvent cleaned quartz substrates. A spin-coating system (G3P SPINCOAT, from Cookson Electric Equipment) at 3000 rpm was used to obtain the thin films. The spin-coating parameters were optimized in order to produce roughly homogenous thickness thin films of approximately 100 nm. The squaraine spin-coated substrates were vacuum dried for several hours to remove residual solvent prior to performing UV-vis spectroscopic and other measurements.

3.3.2 Spectroscopic Measurements

UV-vis absorption measurements of the spin-coated thin films were recorded using an Agilent 8453 (Agilent Technologies). A solid state holder was constructed to accommodate the spin-coated thin film samples. The holder was equipped with heating elements and a temperature control device to allow the measurement of absorption spectra at different temperatures.

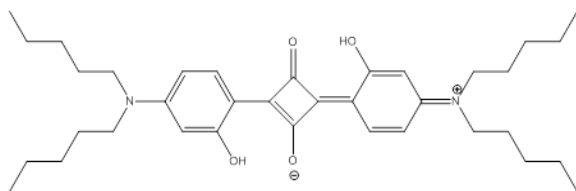
Two types of experiments were carried out. The first one involved the heat treatment of the spin-coated substrates at different temperatures from room temperature to 70 °C (after initial room temperature spin coating) and recording the UV-vis absorption spectrum at each temperature. The second experiment was performed at by holding the spin-coated thin film at a constant temperature (60 °C) and recording the absorption spectrum from 0 to 145 s in 10 s intervals.

3.4 Results and Discussion

To our knowledge, no study has been reported on the effect of temperature on both H- and J- aggregates of squaraine dye derivatives in solid state thin films.

In this study, the results of the investigation and measurements of kinetic properties of J- aggregates for spin-coated films on quartz substrates are presented.

Scheme 3.1 depicts the chemical structure of the squaraine dye derivative, **SQC5(OH)₂**, used to conduct the kinetic study.



Scheme 3-1: Molecular structure of squaraine dye derivative, **SQC5(OH)2** used to study the kinetics of J-aggregates.

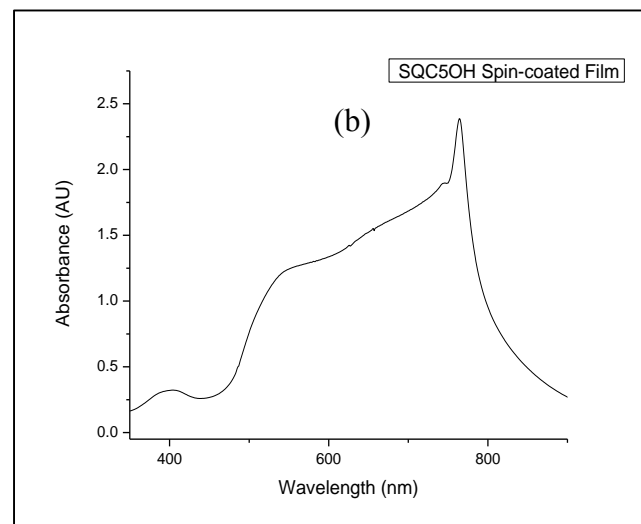
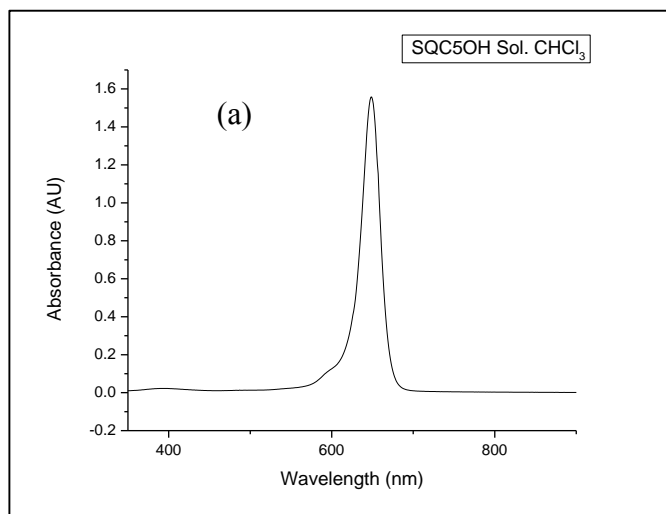


Figure 3-1: UV-vis absorption of SQC5(OH)2 in chloroform solution. (b) UV-vis absorption of SQC5(OH)2 spin-coated thin film.

Figure 3.1 (a) shows the absorption of 1% weight solution in chloroform. The maximum absorption band was observed at 650 nm. Figure 3.1 (b) shows the absorption spectrum of the spin-coated film of the squaraine dye derivative, **SQC5(OH)2**, at room temperature, revealing that two aggregates appear to be formed; one a broad, low intensity blue-shifted (560 nm) H-aggregate and a sharper high intensity red-shifted (767 nm) J-aggregate.

The J-aggregate decays with increasing temperature as shown in Figure 3.2 (a) and with time as in Figure 3.2(b). The decay of the J-aggregate with formation of the H-aggregate are both temperature and time dependent.

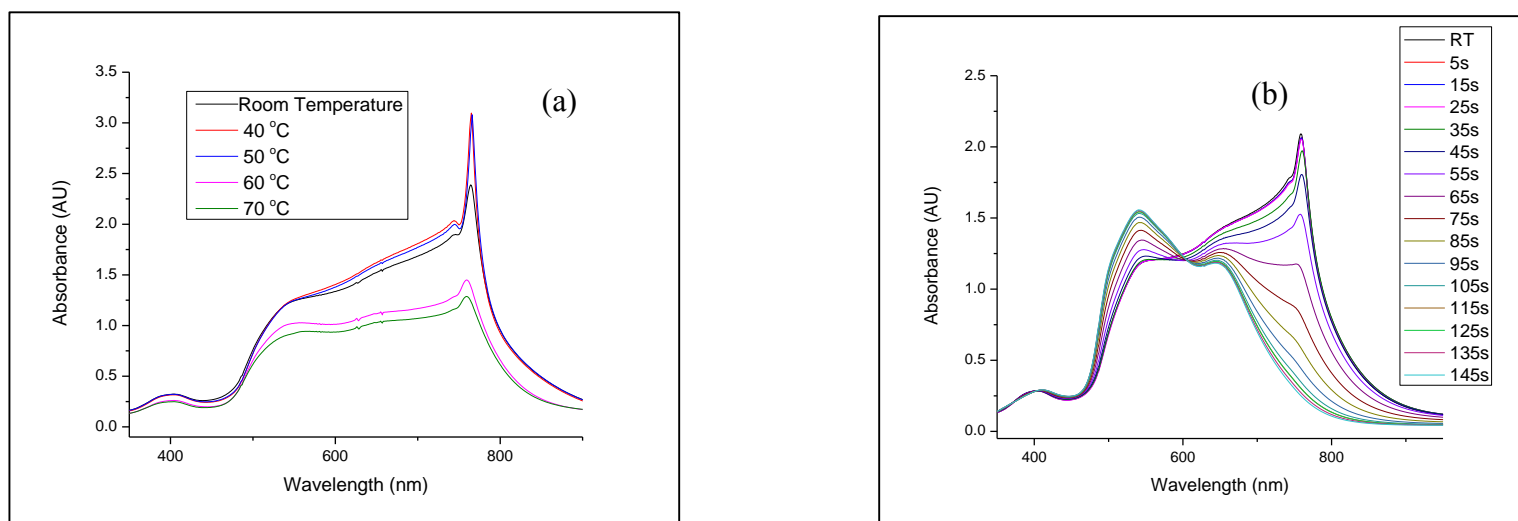


Figure 3-2: (a) The effect of temperature on optical absorption of a SQC5(OH)2 spin-coated film with increasing temperature. (b) Time dependent optical absorption of a SQC5(OH)2 spin-coated film at 60 °C.

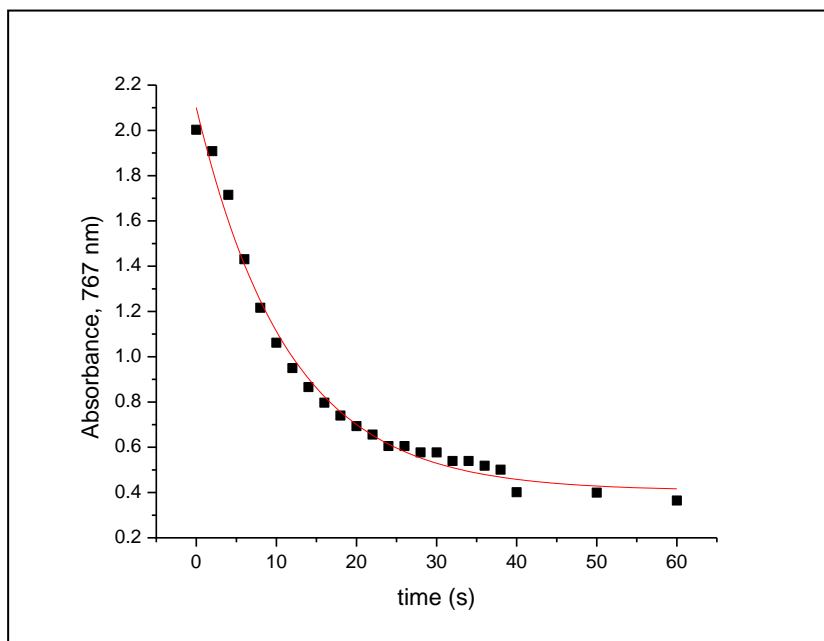


Figure 3-3: Plot of optical absorption of SQC5(OH)₂ spin-coated film at 767 nm vs. time in seconds.

The rate of transformation was evaluated from the change in absorbance of the J-aggregate at 767 nm. Figure 3.3 was used to calculate the rate constant. The experimental points of this curve were best fitted the following equation⁶⁹.

$$Y = Y_0 + Y_1 \exp(-kt)$$

where Y_0 , and Y_1 , are constants, and k is the rate constant of the transformation.

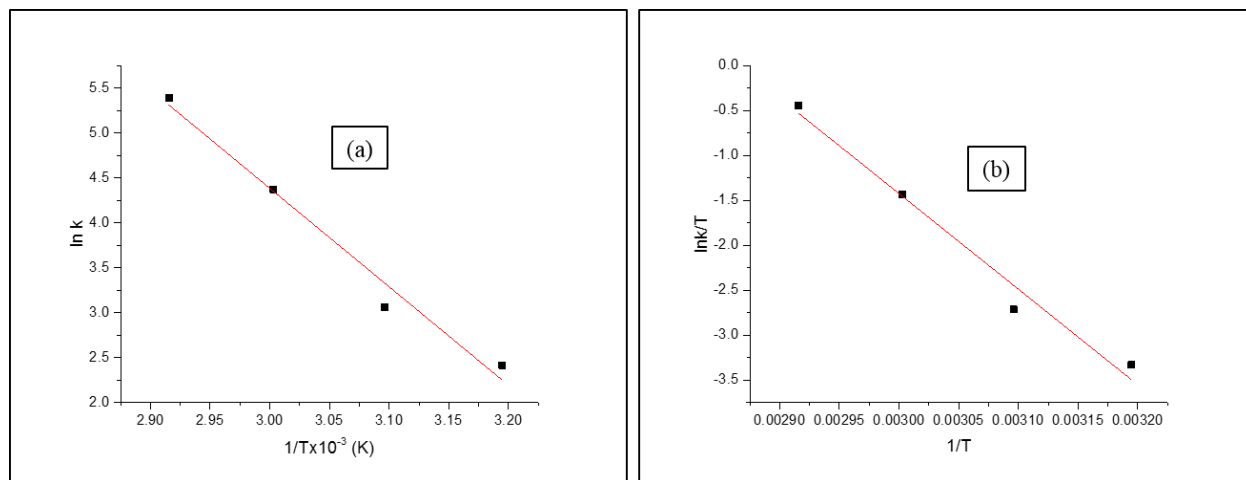


Figure 3-4: (a) Plot of $\ln k$ vs. $1/\text{temperature (K} \times 10^{-3})$. (b) Plot of $\ln k/T$ vs. $1/\text{temperature}$.

Table 3-1: Kinetics data of SQC5(OH)2 transformation

1/T	ln k	lnk/T
3.194888	2.415914	-3.33029
3.095975	3.063391	-2.71426
3.003003	4.374498	-1.43364
2.915452	5.393173	-0.44456

The activation energy (E_a) of the decay of the J-aggregate was calculated using the Arrhenius Equation $k = Z e^{-E_a/RT}$.

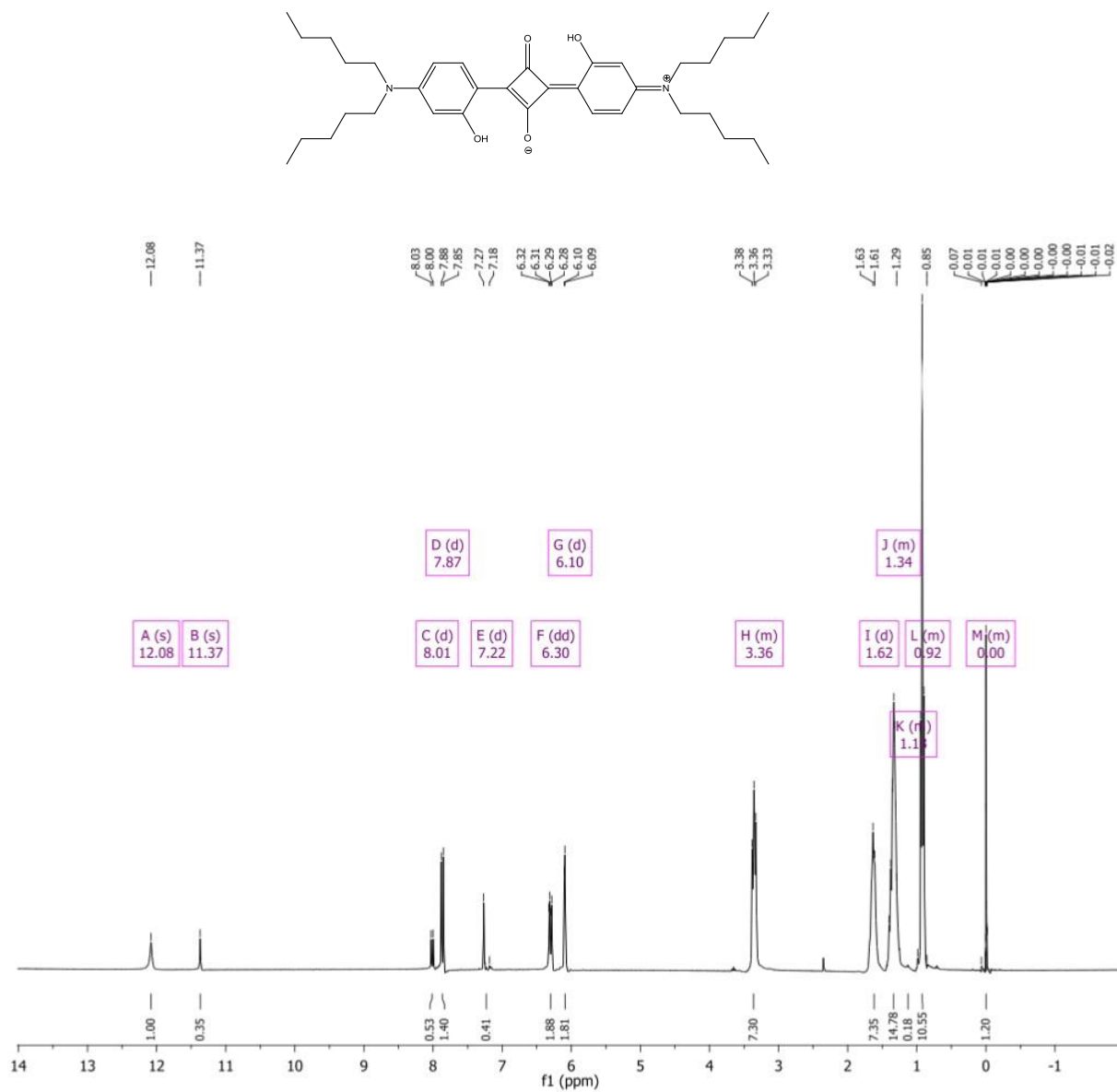
where Z = pre-exponential factor, E_a = activation energy, R = gas constant, $8.314 \text{ JK}^{-1}\text{mol}^{-1}$, and T = temperature in kelvin. The value of this activation energy was calculated as 91.2 kJ. The enthalpy and entropy of the J-aggregate decay process were calculated using Eyrin equation $k = k_B/h e^{-\Delta G/RT}$, where k is the rate constant of the process, k_B is the Boltzmann's constant, h is the Plank's constant, T is temperature in kelvin. The calculated ΔH and ΔS were 88.4 kJ/mol and 48.2 J/K mol, respectively.

3.5 Conclusion

Kinetic investigation and studies of spin-coated films a squaraine derivative J-aggregate revealed that this type of aggregation is formed upon spin-coating on glass substrates. The studies have elucidated that the formed J-band (767 nm) decays upon heat treatment. The decay of the J-aggregate is accompanied with the formation and enhancement of a blue-shifted band that absorbs in visible region at 560 nm. The J-aggregate decay process is temperature and time dependent. It increases with increasing temperature and time. The absorption vs. heat treatment approach described in this work shows that heat treatment may be used to modify the properties of the spin-coated film and that the initial J-aggregate appears to be the kinetic product while the H-aggregate is the thermodynamically more favorable aggregate. This study and investigation of the spin-coated film showed that kinetic features such as the activation energy along with the enthalpy and entropy of the decay of J-aggregate can obtained from the rate constant of the process. This also indicates that it is possible to modulate optical properties of squaraine-aggregate thin films via processing conditions.

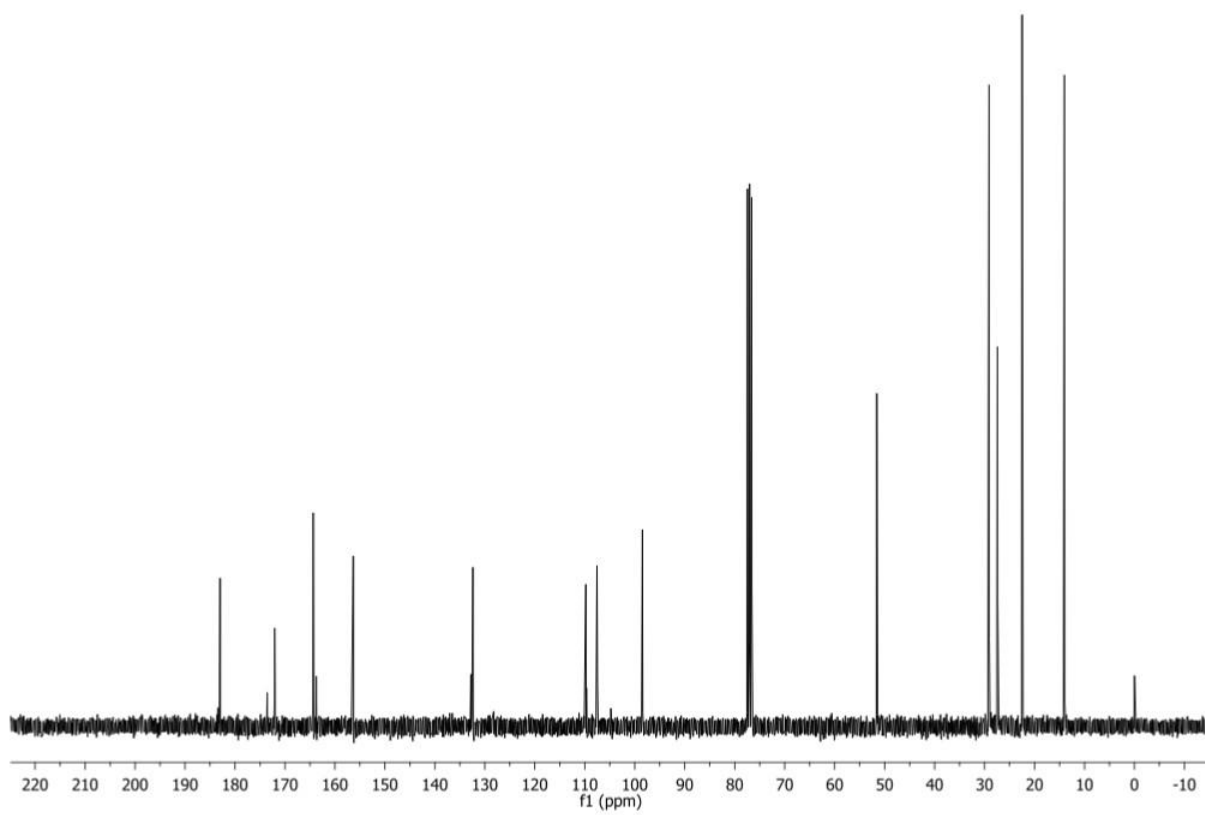
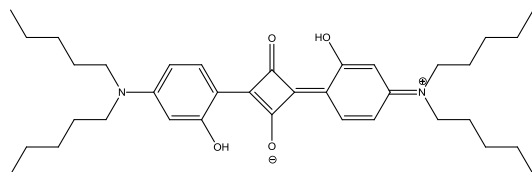
APPENDIX A: ^1H AND ^{13}C NMR SPECTRA OF SQUARINE DERIVATIVES

¹H NMR OF SQC5(OH)2



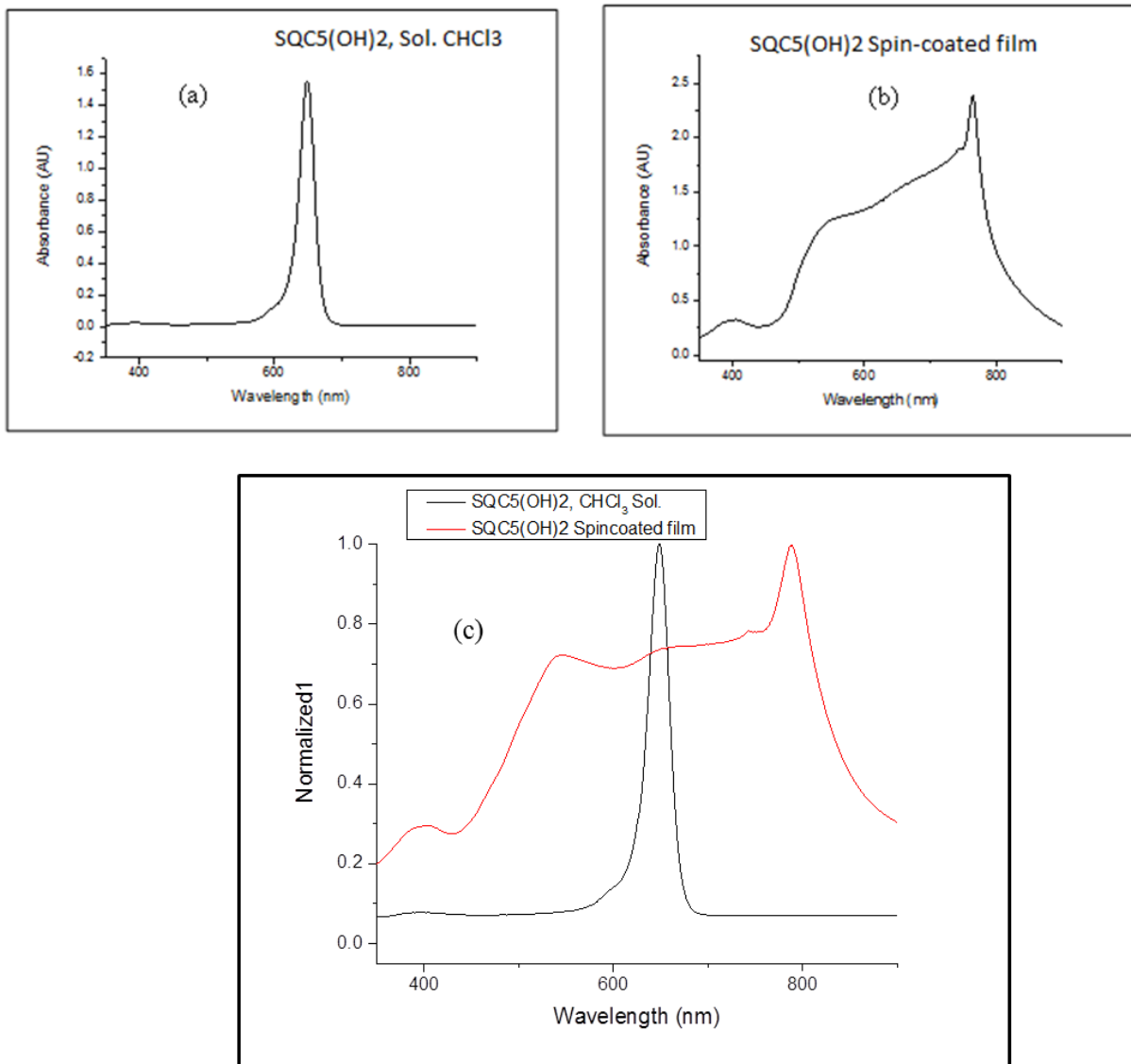
¹H NMR: 2, 4-Bis [4-(N, N-(di-n-pentylamino)-2-hydroxyphenyl] squaraine, SQC5(OH)2.

^{13}C NMR OF SQC5(OH)2

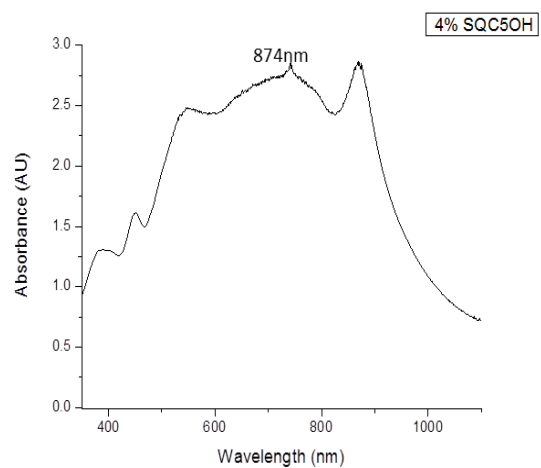
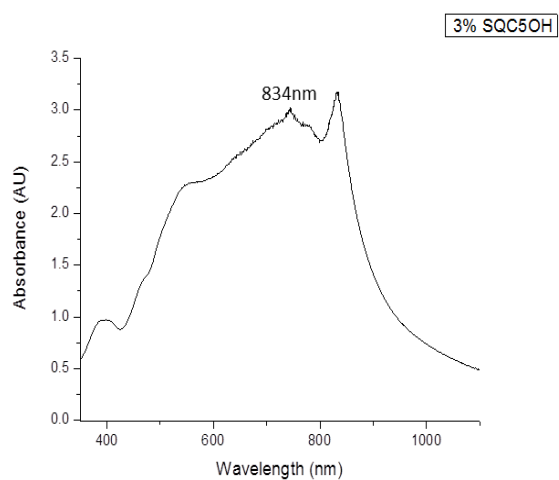
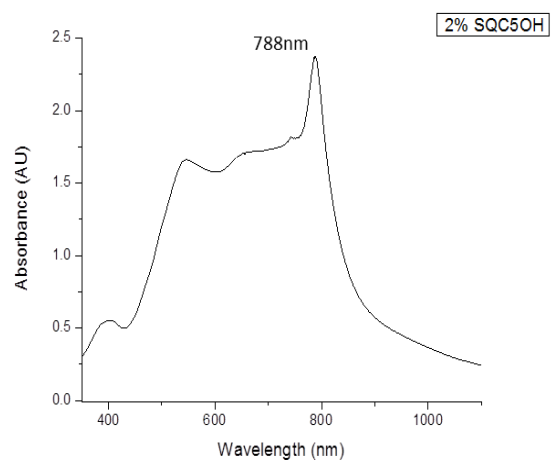
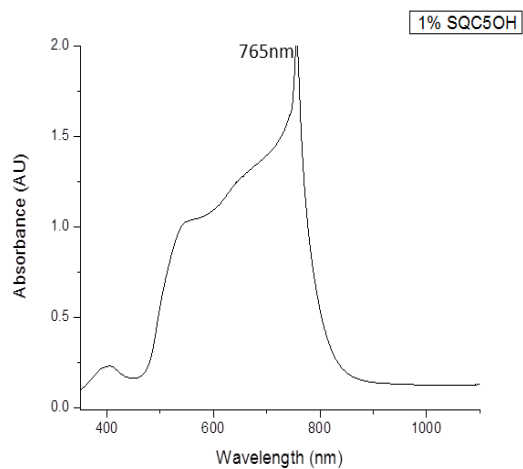


^{13}C NMR: 2, 4-Bis[4-(*N,N*-(di-*n*-pentylamino)-2-hydroxyphenyl] squaraine, SQC5(OH)2.

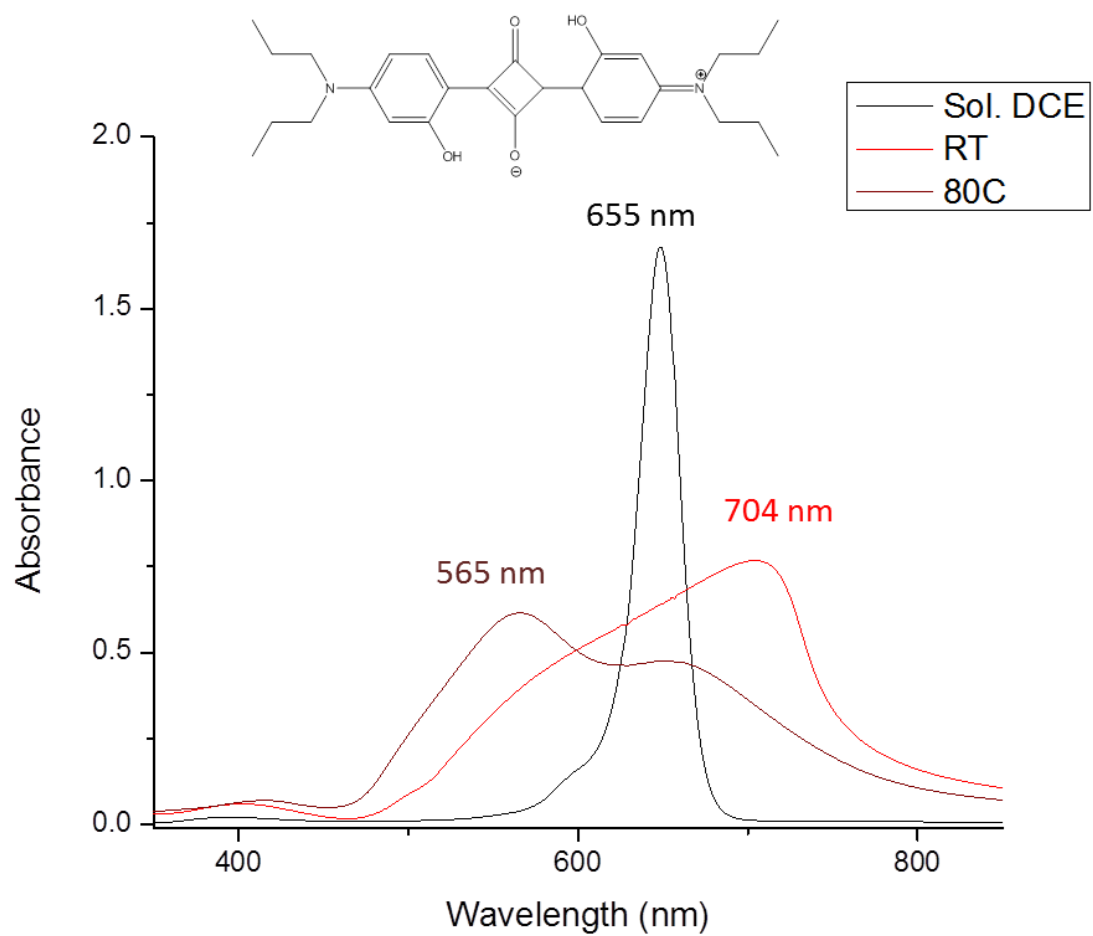
APPENDIX B: UV-VIS SPECTRAL DATA



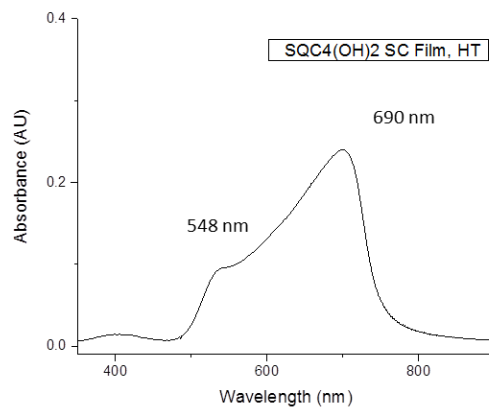
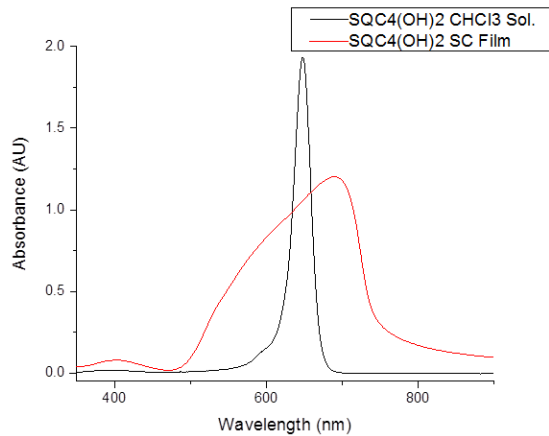
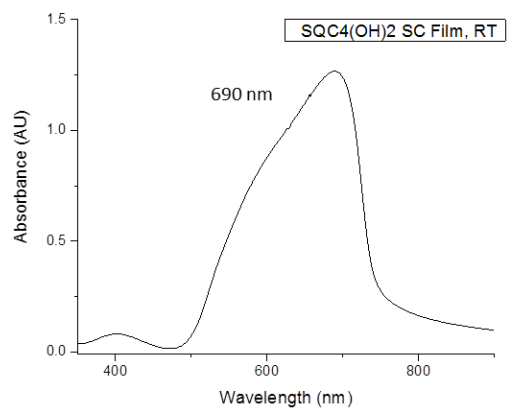
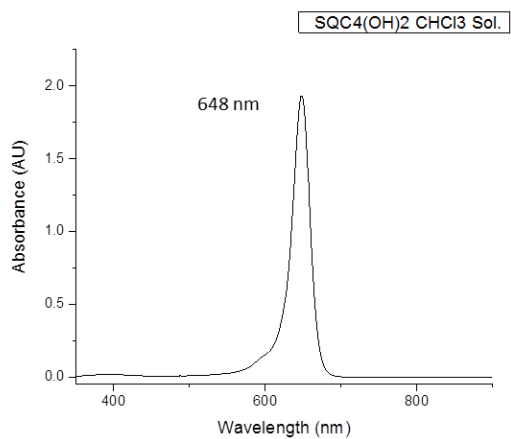
SQC5(OH)2 dye spectra: (a) spectrum of SQC5(OH)2 in chloroform diluted solution, (b) spectrum of the SQC5(OH)2 spin-coated thin film, (c) absorption bands of liquid and solid states.



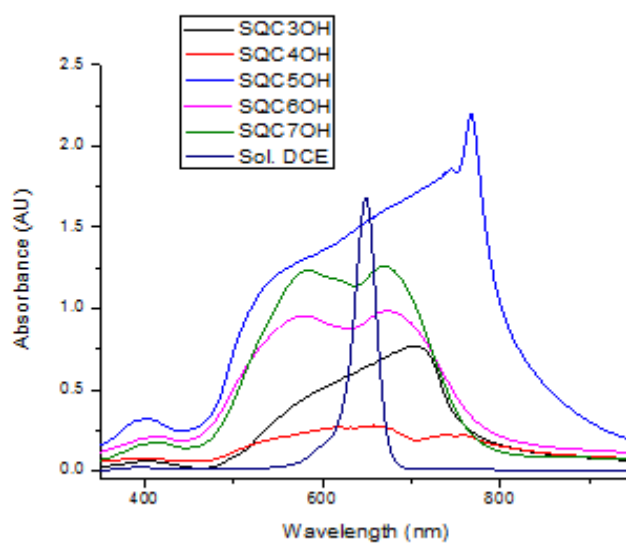
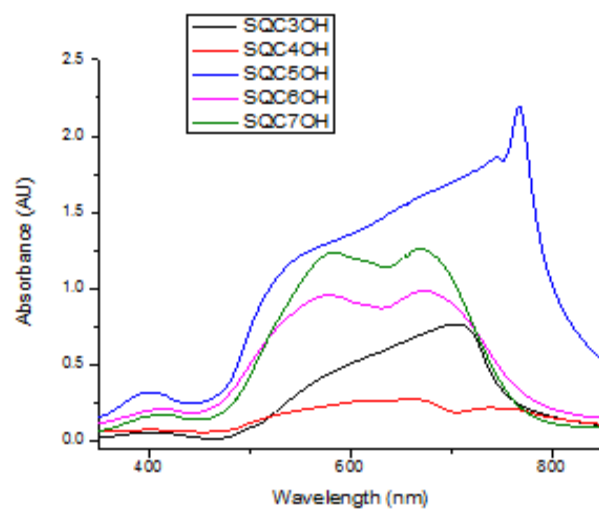
Effect of concentration (% w/w) on the J-aggregates in spin coated thin film for squaraine dye
SQC5(OH)₂



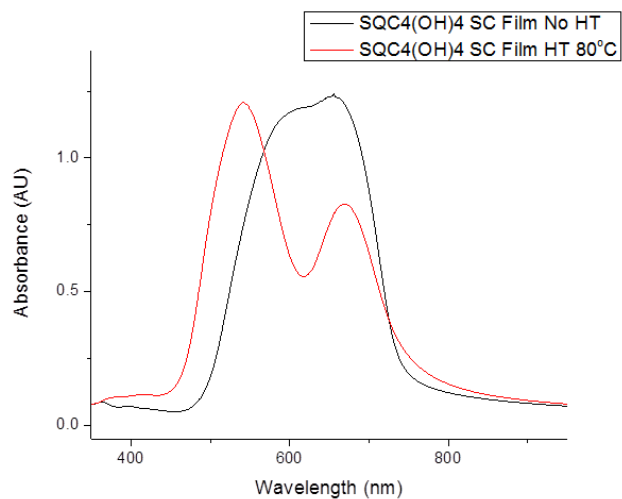
SQC3(OH)₂ dye spectra in dilute solution, spin-coated thin film at room temperature, and spin-coated film after heat treated at 80 °C.



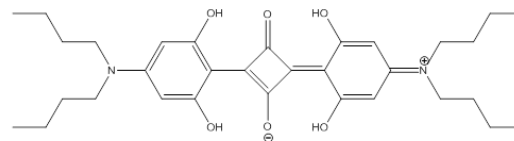
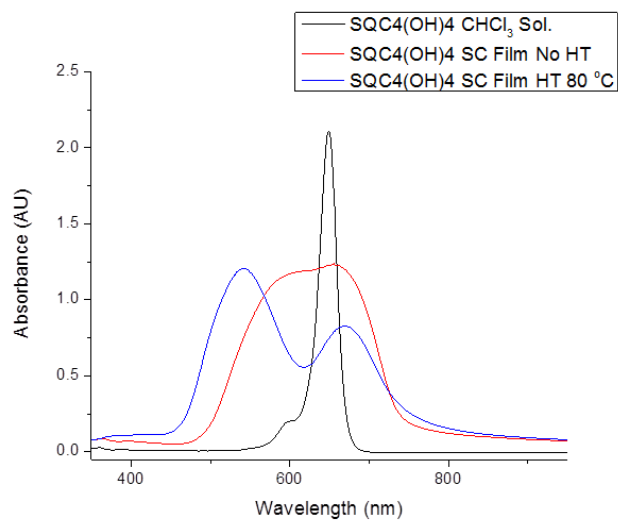
UV-vis spectra of the squaraine dye SQC4(OH)₂



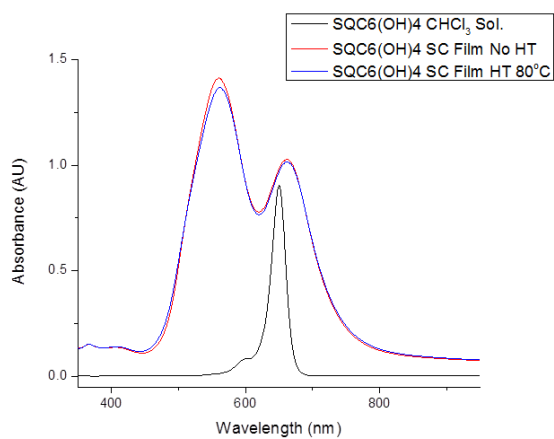
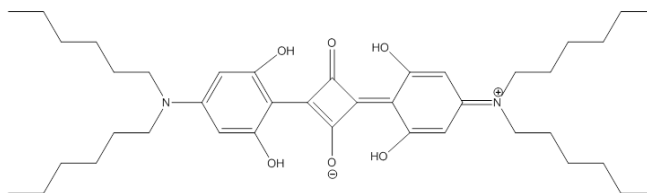
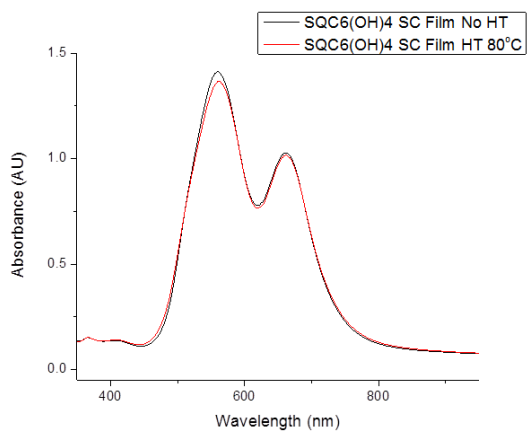
UV-vis absorption spectra of SQCX(OH)₂ series



SQC4(OH)4

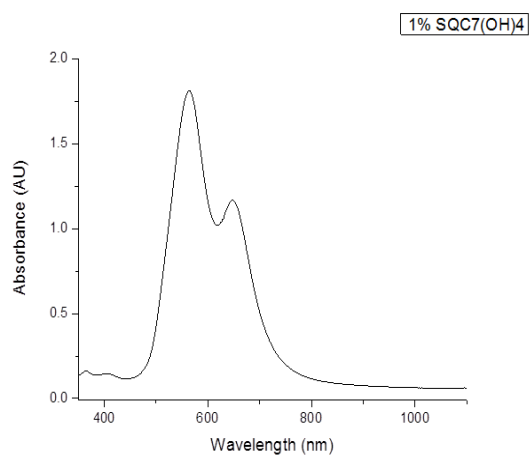


UV-vis spectra of the squaraine dye SQC4(OH)4

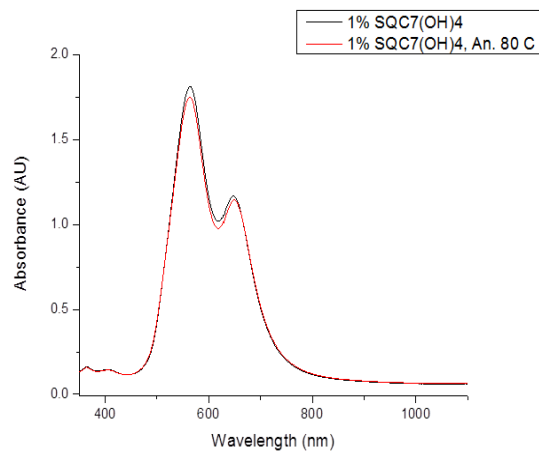
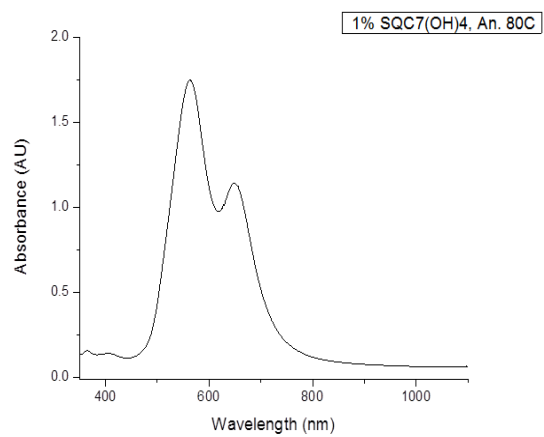
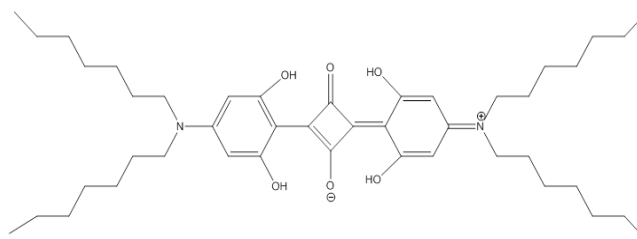


SQC6(OH)4

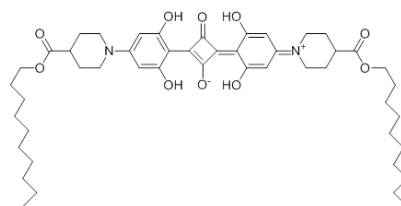
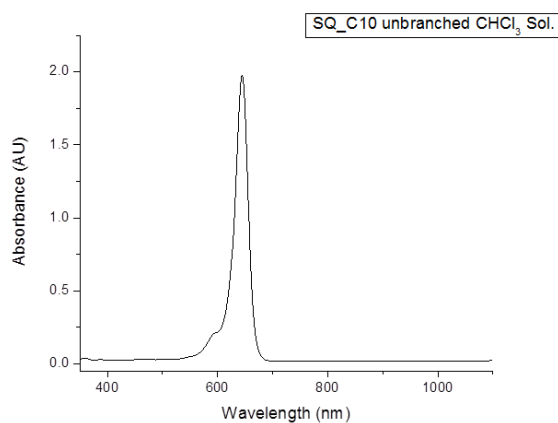
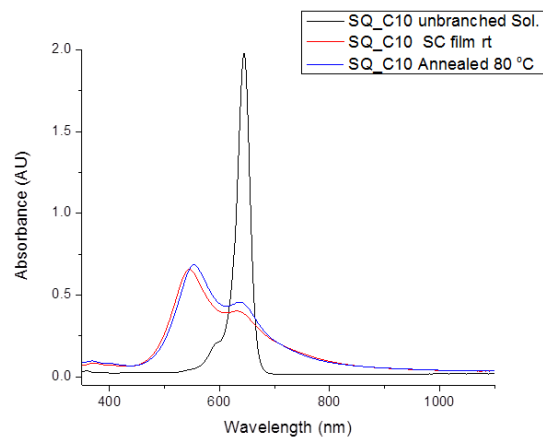
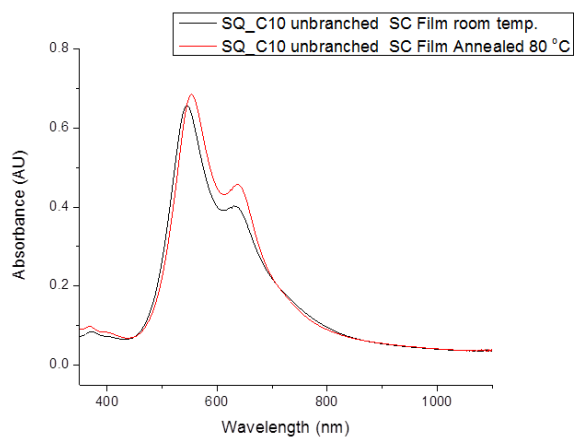
UV-vis spectra of the squaraine dye SQC6(OH)4



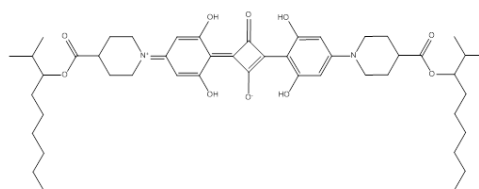
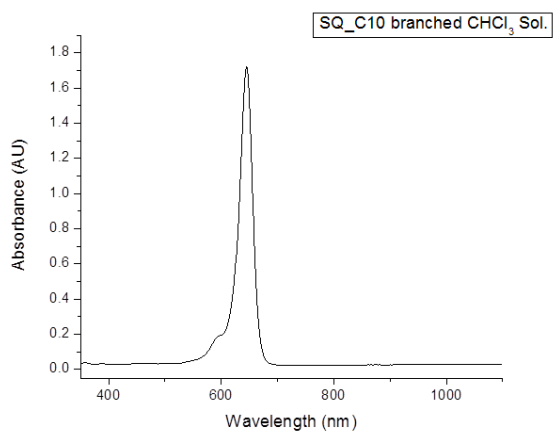
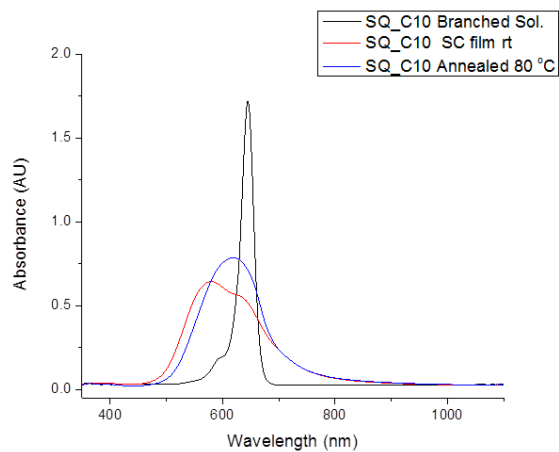
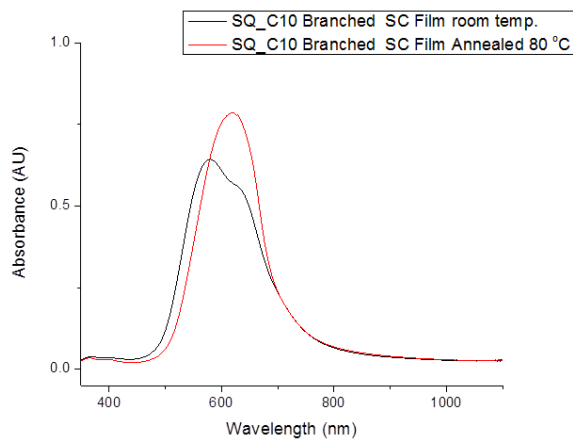
SQC7(OH)4



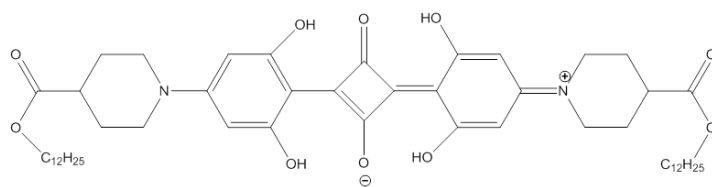
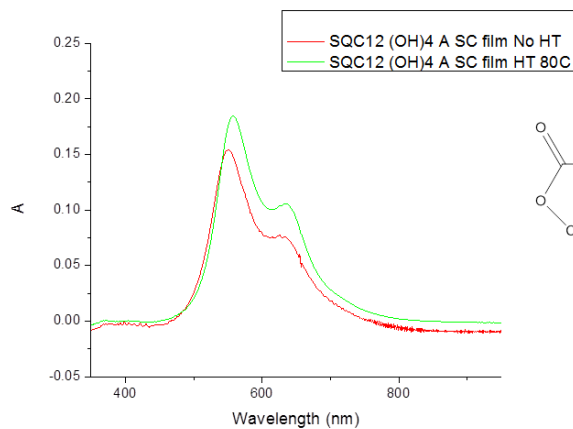
UV-vis spectra of the squaraine dye SQC7(OH)4



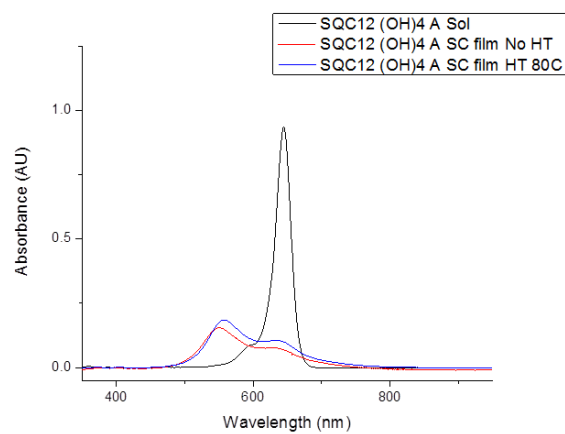
UV-vis spectra of the squaraine dye SQ10(OH)₄ n



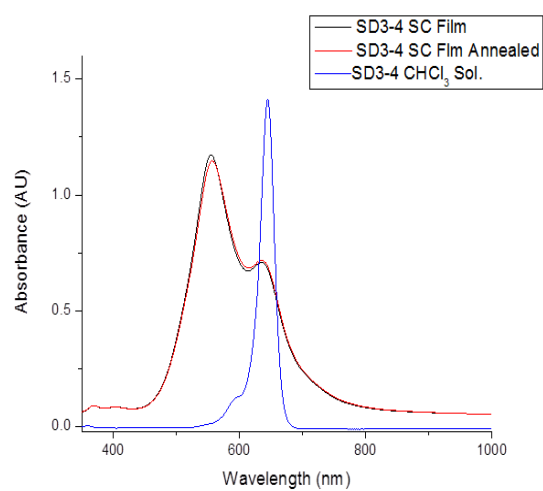
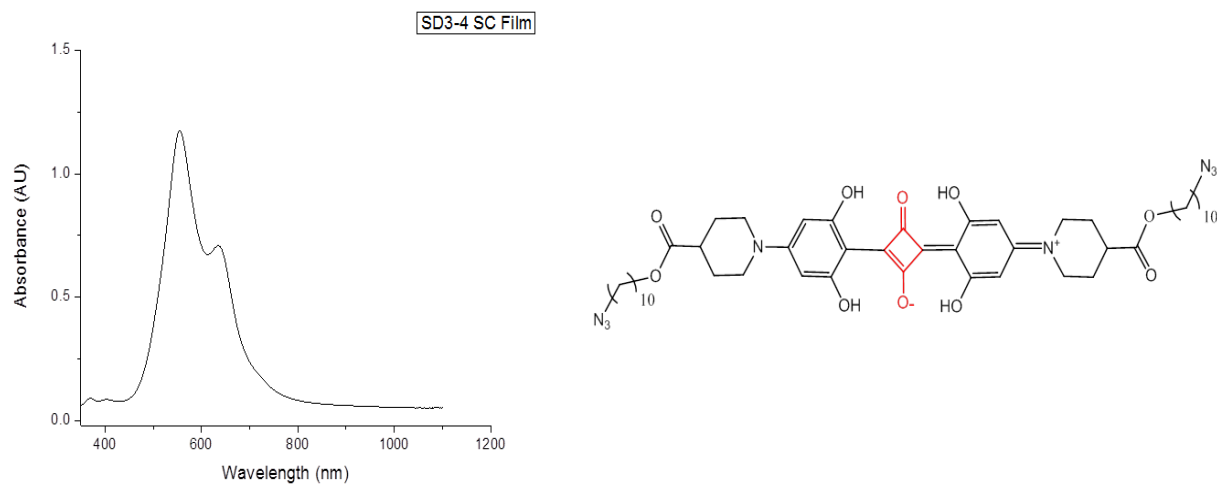
UV-vis spectra of the squaraine dye SQ10(OH)₄ b



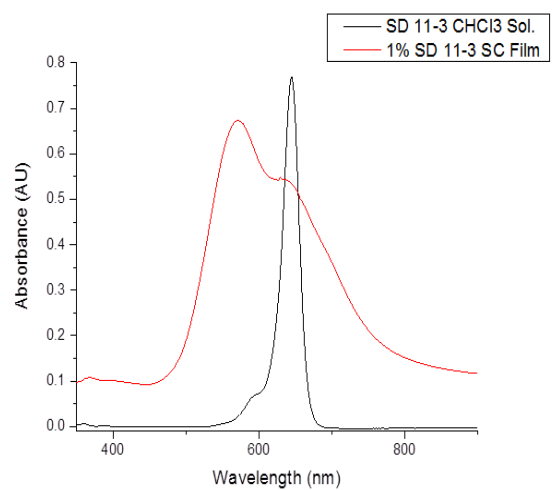
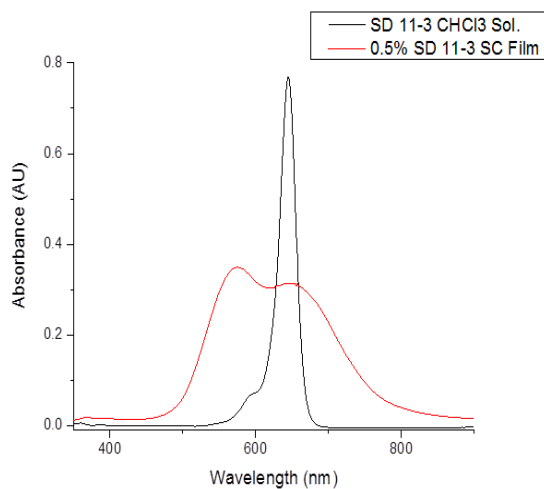
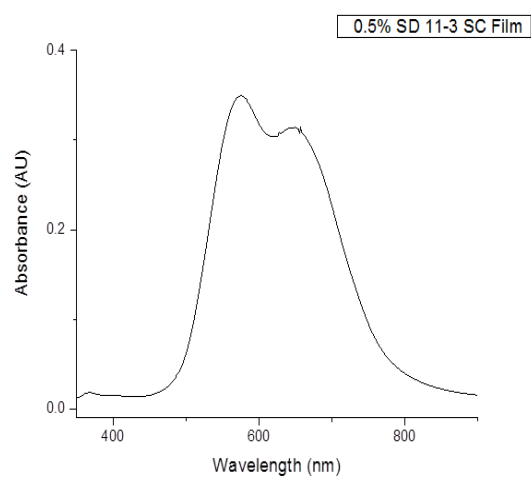
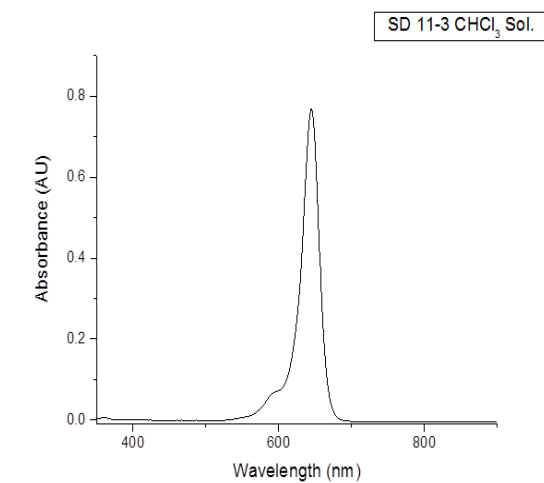
SQC12Ac(OH)4



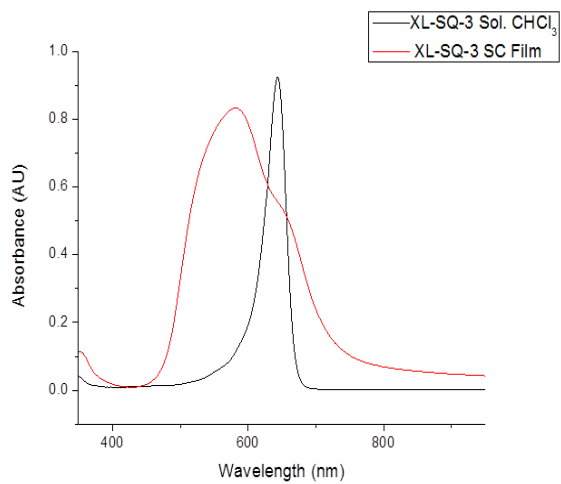
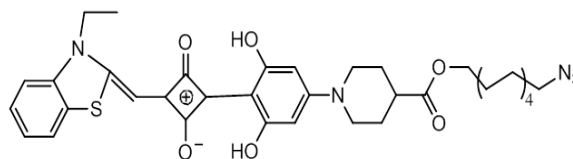
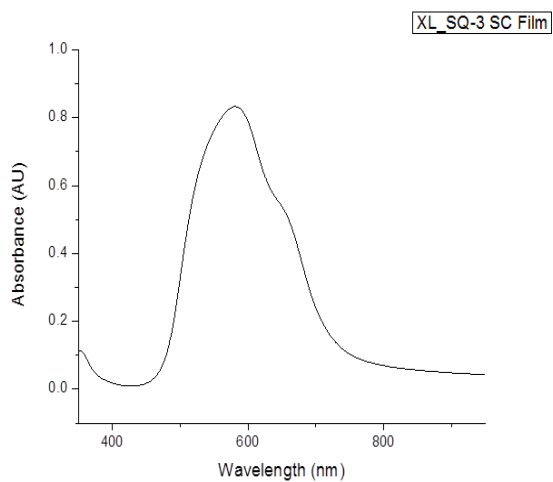
UV-vis spectra of the squaraine dye SQC12Ac(OH)4



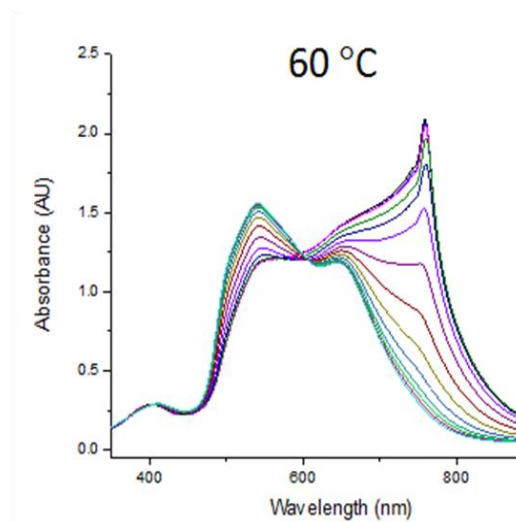
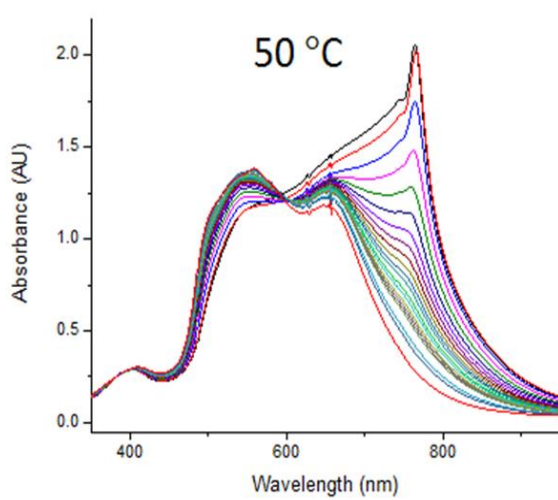
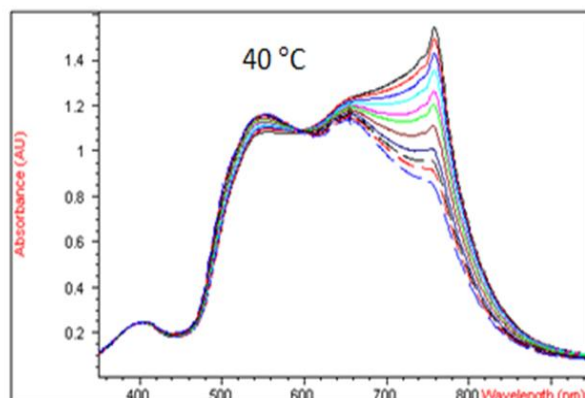
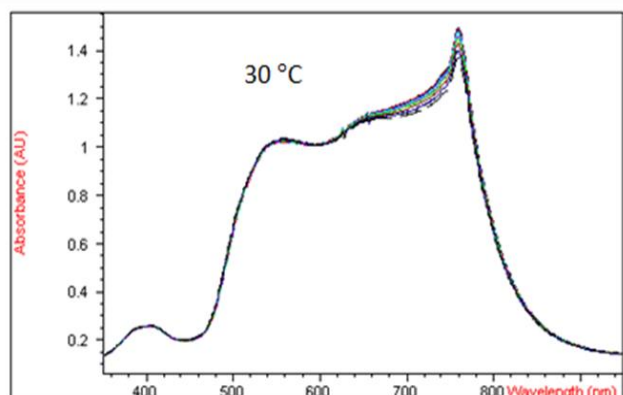
UV-vis spectra of the squaraine dye SD3-4



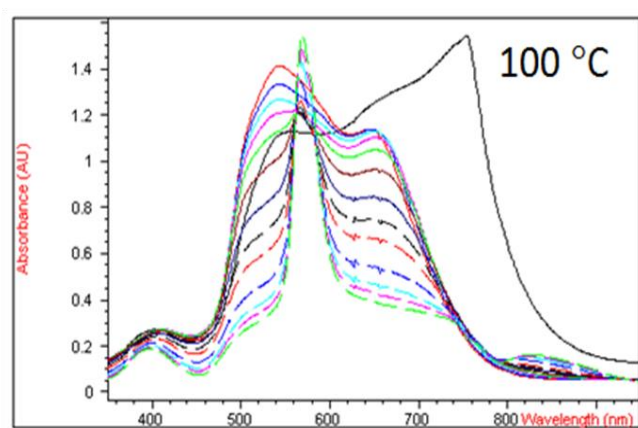
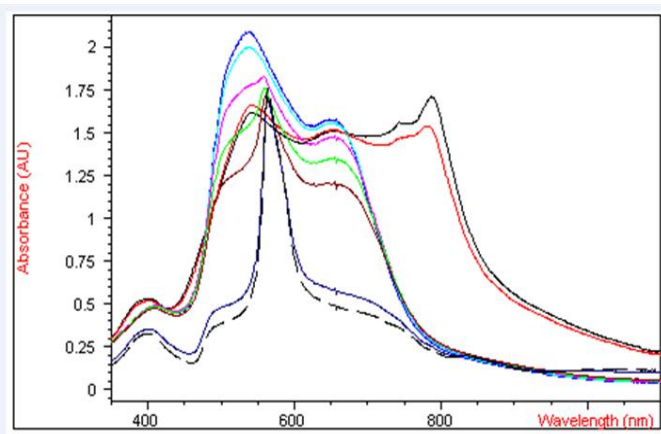
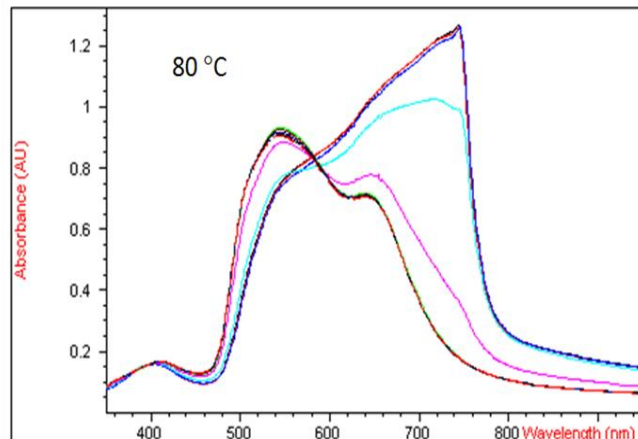
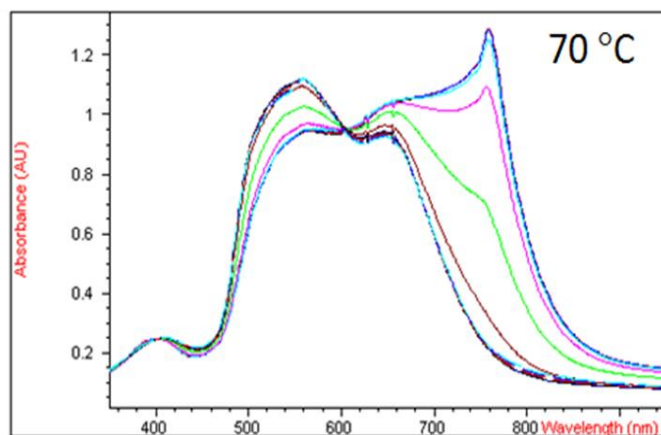
UV-vis spectra of the squaraine dye SD11-3



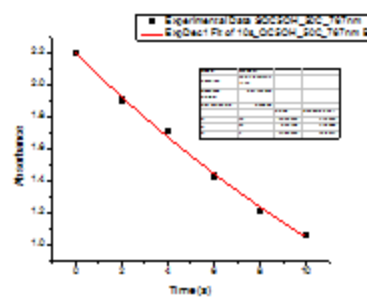
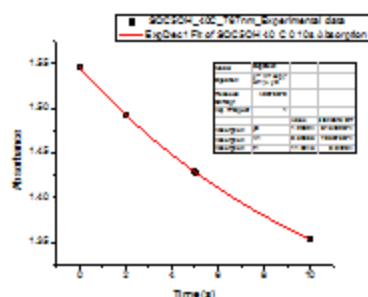
UV-vis spectra of the squaraine dye XL SQ-3



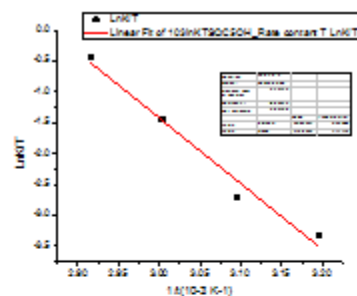
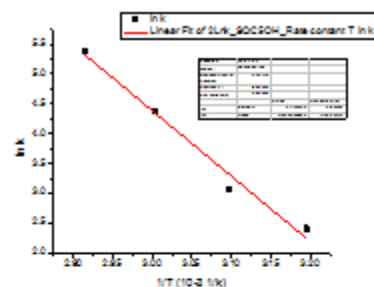
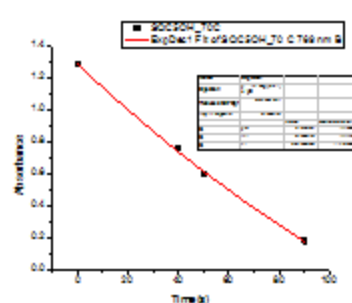
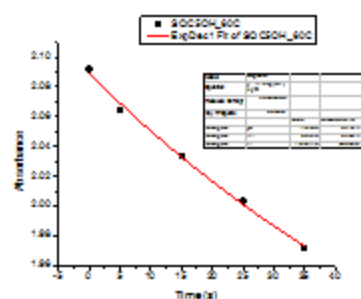
UV-vis absorption of SQC5(OH)₂ spin-coated films recorded at different temperatures (30 °C-60 °C)



UV-vis absorption of SQC5(OH)₂ spin-coated films recorded at different temperatures (70 °C-100 °C)



Kinetic of J-aggregation : SQC5OH Squaraine dye



$$K = Z \exp^{-E_a/RT}$$

$$\ln k = -E_a/R[1/T] + \ln Z$$

$$E_a = 91.2 \text{ kJ/mol}$$

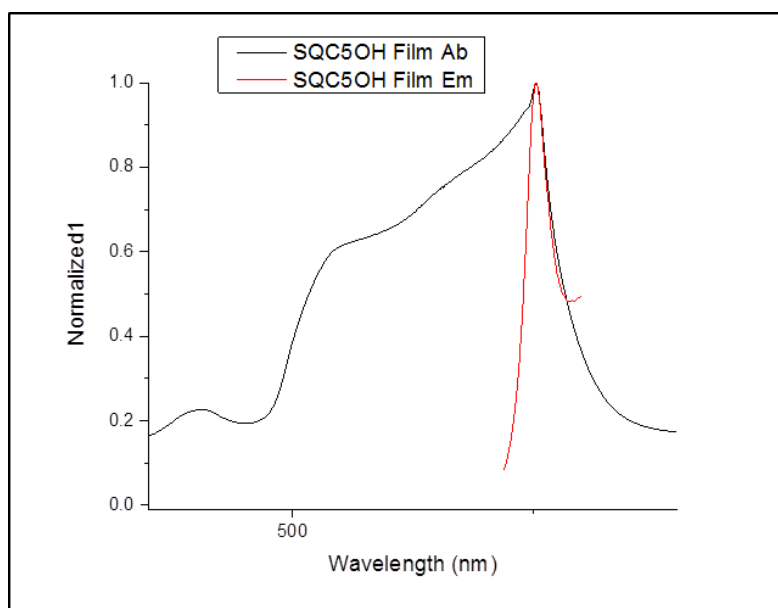
$$K = k_B/h \exp^{-\Delta G/RT}$$

$$\ln k/T = -\Delta H/R[1/T] + \ln k_B/h + \Delta S/R$$

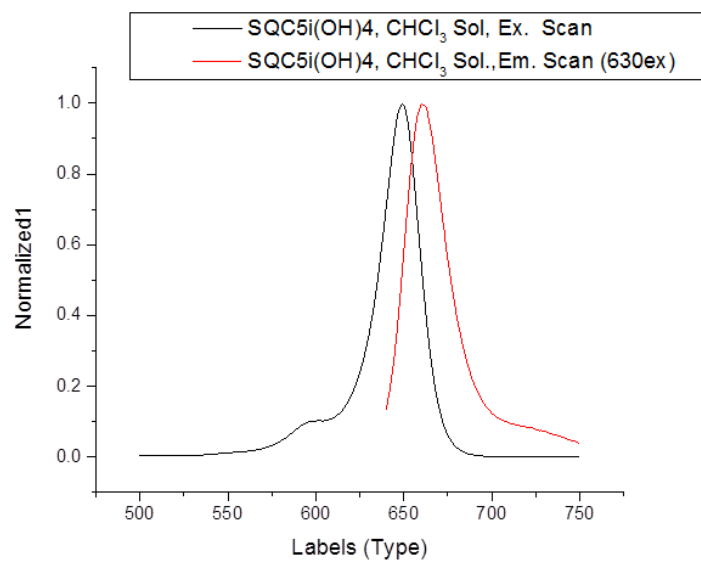
$$\Delta H = 88.4 \text{ kJ/mol}$$

$$\Delta S = 48.2 \text{ J/K.mol}$$

APPENDIX C: PHOTOLUMINESCENCE SPECTRAL DATA

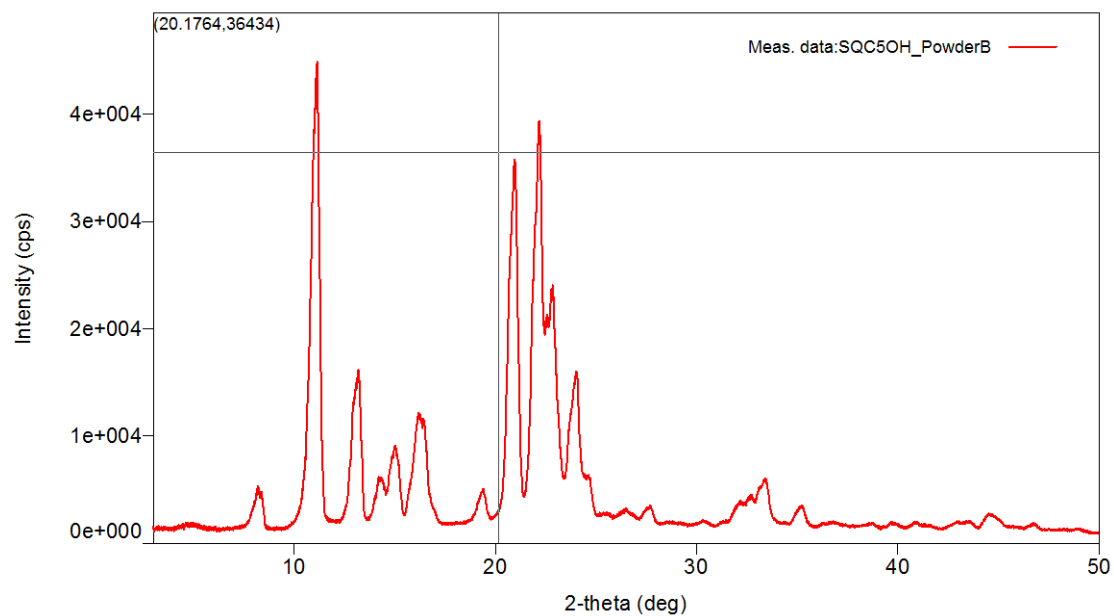


Absorption and emission spectra of SQC5(OH)2 thin film spin-coated from 1% w/w chloroform solution

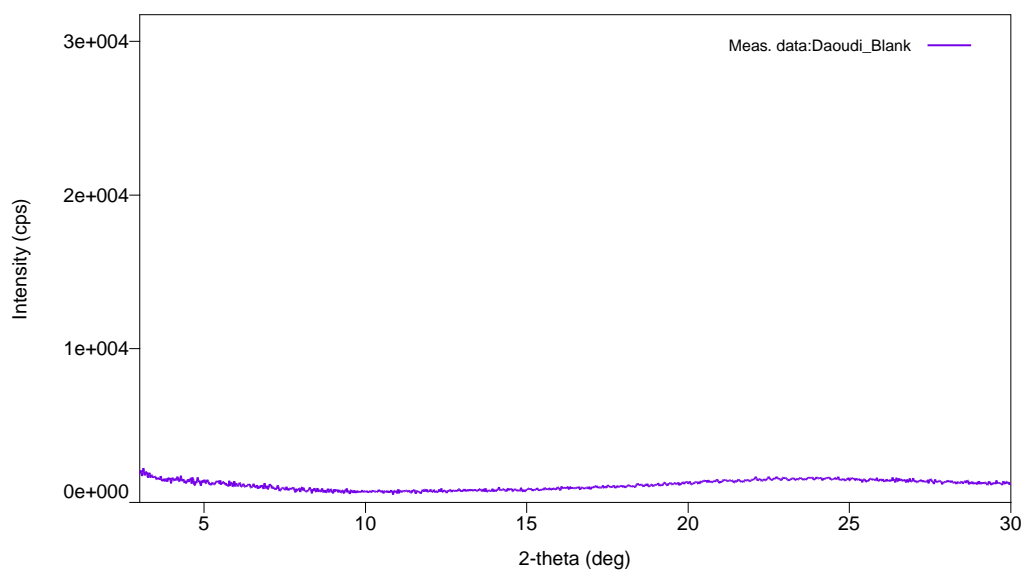


Absorption and emission spectra of SQC5(OH)4 b in dilute chloroform solution

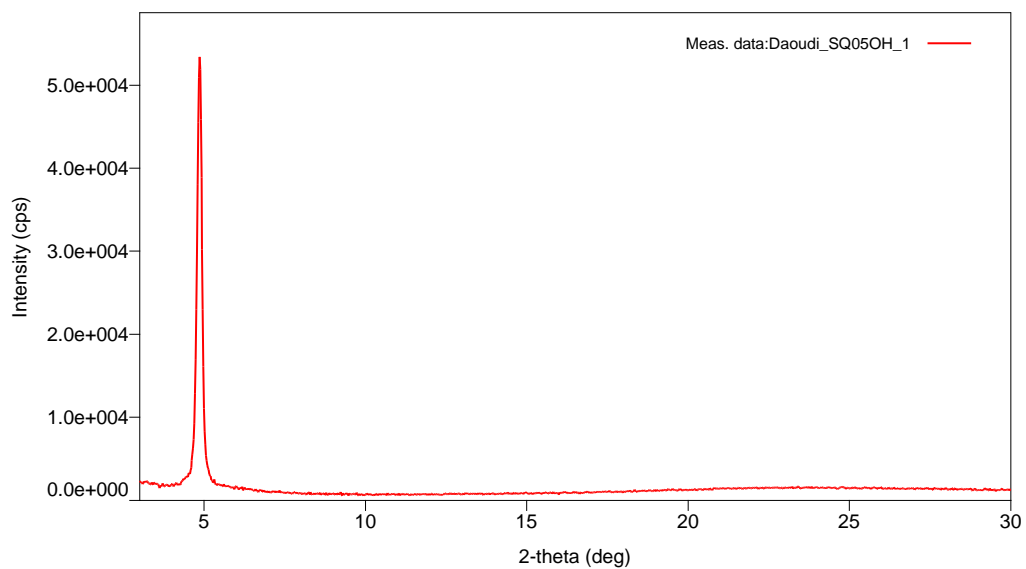
APPENDIX D: X-RAY DIFFRACTION DATA



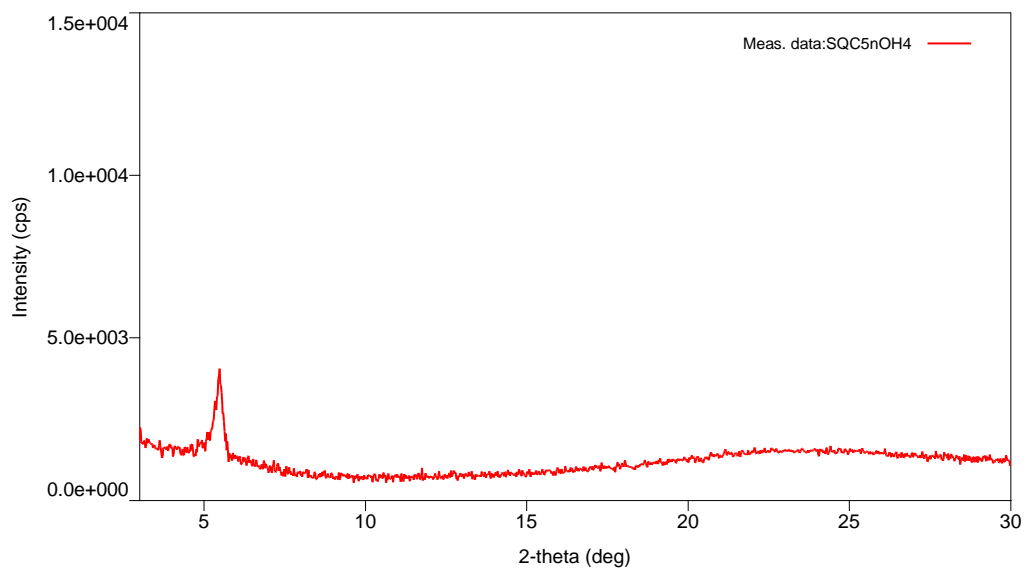
X-ray diffraction patterns of 2,4-bis [4-(N,N-di-n-pentylamino)-2-hydroxyphenyl] squaraine, (SQC5OH)₂.powder



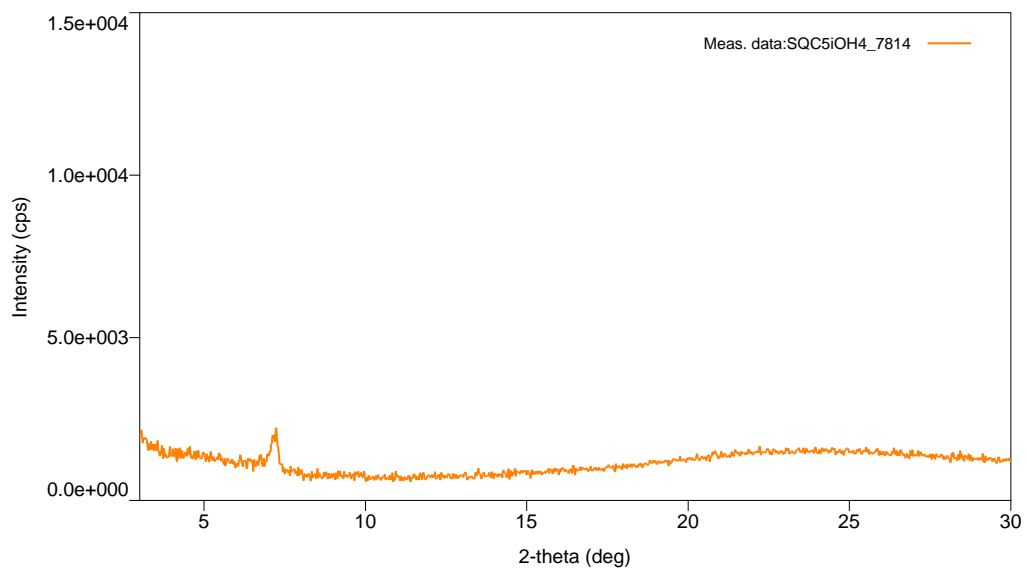
X-ray diffraction patterns of glass substrate (blank)



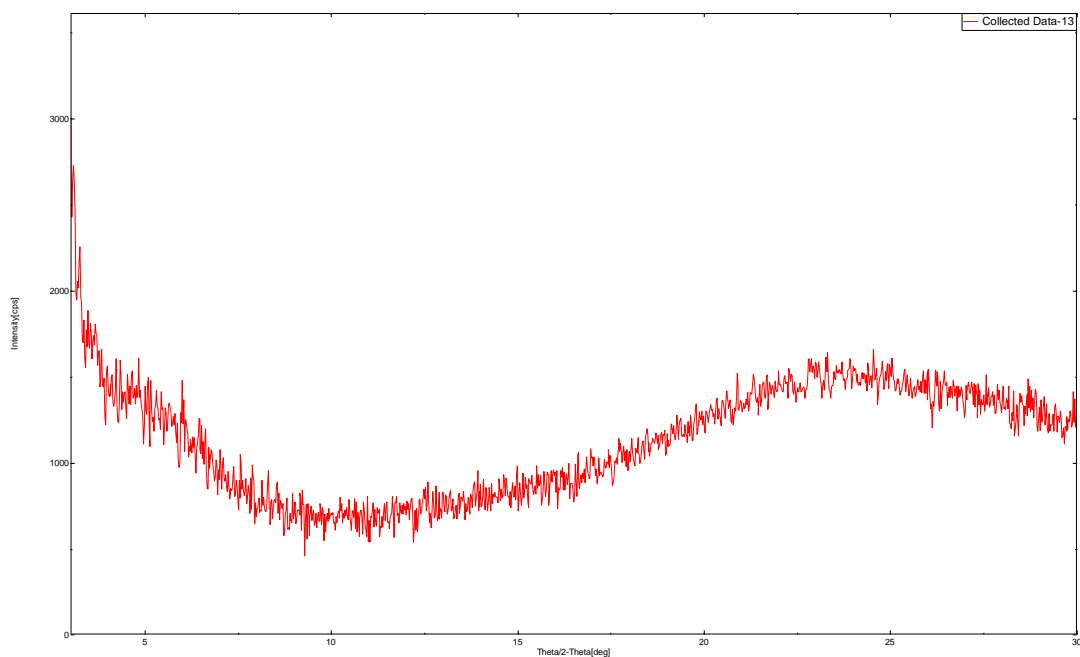
X-ray diffraction patterns of 2,4-bis [4-(N,N-di-n-pentylamino)-2-hydroxyphenyl] squaraine, [SQC5OH]₂.spin-coated thin film



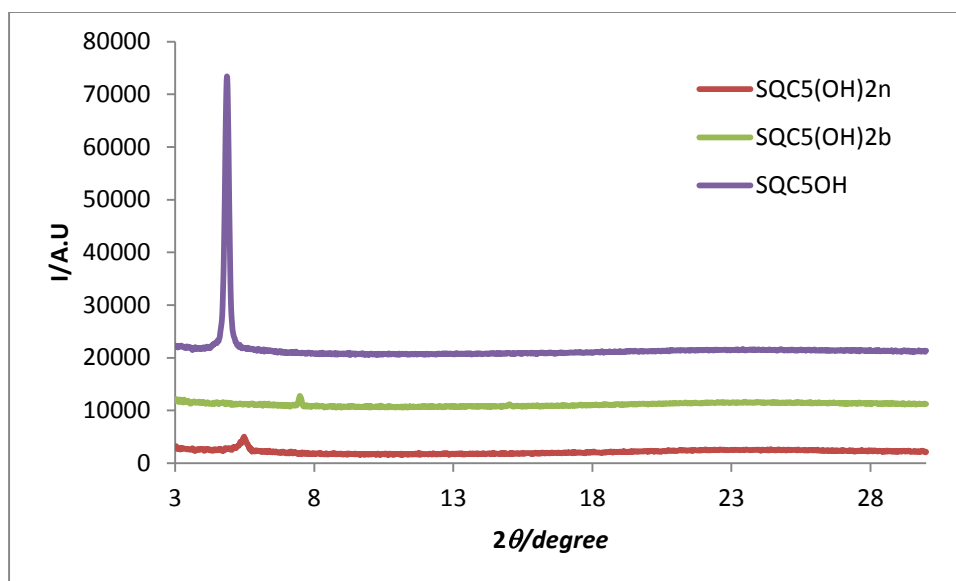
X-ray diffraction patterns of 2,4-bis [4-(N,N-di-n-pentylamino)-2-hydroxyphenyl] squaraine, (SQC5(OH)₄).thin film



X-ray diffraction patterns of 2,4-bis [4-(N,N-di-n-pentylamino)-2-hydroxyphenyl] squaraine, [SQC5(OH)4b].thin film

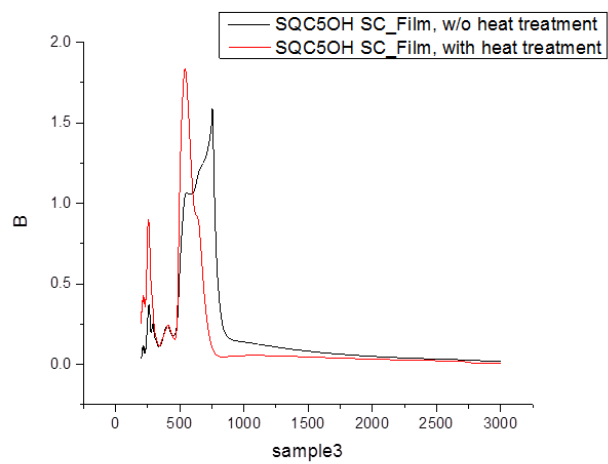
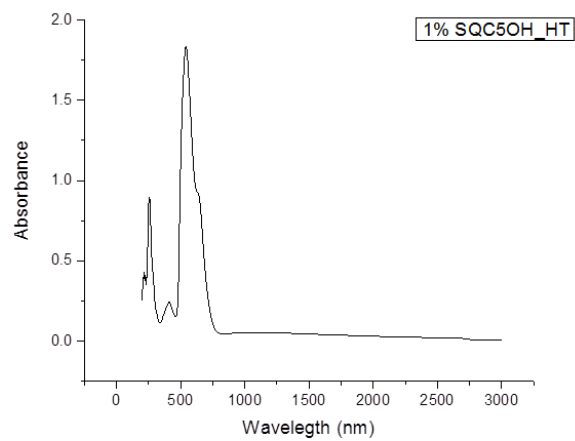
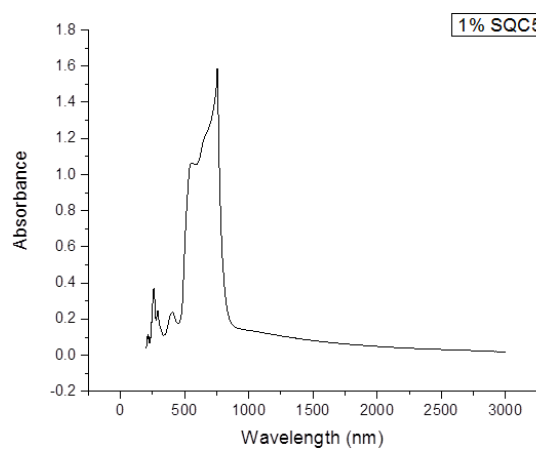


X-ray diffraction patterns of SD11-4(OH)4].thin film



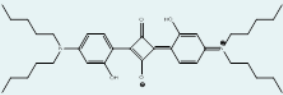
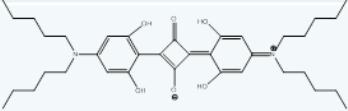
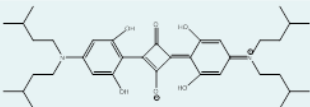
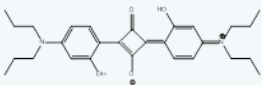
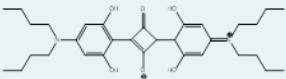
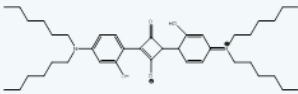
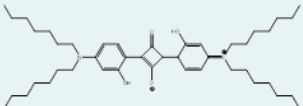
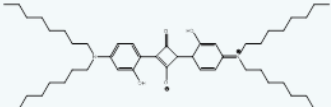
X-ray diffraction patterns of squaraine dyes, SQC5(OH)₂, SQC5(OH)₄ n, and SQC5(OH)₄ b spin-coated thin film

APPENDIX E: NIR SPECTRAL DATA



NIR Absorption Spectra of Squaraine Dye SQC5(OH)₂.

List of squaraine dye structures

Dye	Structure
SQC5(OH) ₂	
SQC5(OH) ₄ n	
SQC5(OH) ₄ b	
SQC3(OH) ₂	
SQC4(OH) ₂	
SQC6(OH) ₂	
SQC7(OH) ₂	
SQC8(OH) ₂	

Dye	Structure
SQC12Ac(OH)4	
SQC10(OH)4 b	
SQC10(OH)4 n	
SQC4(OH)4 n	
SQC4(OH)4 b	
SQC6(OH)4	
SD3-4	
SQ-3	
XL- SQ-3	

LIST OF REFERENCES

- (1) Makowski, B. T.; Valle, B.; Singer, K. D.; Weder, C. *J. Mater. Chem.*, **2012**, 22, 2848–2850
- (2) Sleiman, M.H.; Ladame, S. *Chem. Commun.*, **2014**, 50, 5288-5290
- (3) Yan, Z. Q.; Guang, S. Y.; Su, X. Y.; Xu, H. Y. *J. Phys. Chem. C*, **2012**, 116, 8894-8900
- (4) Beverina, L.; Salice, P. *Eur. J. Org. Chem.* **2010**, 1207-1225
- (5) Zhang, Y.; Kim, B.; Yao, C.; Bonder, M. V.; Belfield, K. D. *Langmuir*, **2013**, 29, 11005-11012
- (6) Mayehohoffer, U.; Wurthner, F. *Chem. Sci.*, **2012**, 3, 1215-1220
- (7) Yefimova, S.; Lebed, A.; Sorokin, A.; Guralchuk, G.; Borovoy, I.; Malyukin, Y. *J. Mol. Liq.*, **2012**, 165, 113-118
- (8) Nizamov, Sh. N.; Barakaeva, M. N.; Kurtaliev, E. N.; Tatarets, A. L.; Patsenker, L. D. *J. Appl. Spectrosc.*, **2009**, 76, 464-469
- (9) Alex, S.; Basheer, M. C.; Arun, K. T.; Ramaiah, D.; Das, S. *J. Phys. Chem. A*, **2007**, 111, 3226-3230
- (10) Stoll, R. S.; Severin, N.; Rabe, J. P.; Hecht, S. *Adv. Mater.*, **2006**, 18, 1271-1275
- (11) Liu, D.; Kamat, P. V.; George, M. V. *J. Phys. Chem.*, **1996**, 100, 17310-17317
- (12) Chen, H.; Law, K. Y.; Perlstein, J.; Whitten, D. G. *J. Am. Chem. Soc.*, **1995**, 117, 7257-7258
- (13) Das, S.; Thanulingam, T. L.; Thomas, K. G. *J. Phys. Chem.*, **1993**, 97, 13620-13627
- (14) Xu, Y.; Li, Z.; Malkovskiy, A.; Sun, S.; Pang, Y. *J. Phys. Chem. B*, **2010**, 114, 8574-8580

- (15) Ashwell, G. J.; Berry, M. *J. Mater. Chem.*, **2005**, *15*, 108-110
- (16) Tian, M.; Furuki, M.; Iwasa, I.; Sato, Y.; Pu, L. S.; Tatsuura, S. *J. Phys. Chem. B*, **2002**, *106*, 4370-4376
- (17) Stanescu, M.; Samha, H.; Perlstein, J.; Whitten, D.G. *Langmuir*, **2000**, *16*, 275-281
- (18) Ashwell, G. S.; Williamson, P. C.; Green, A.; Bahrac, G. S.; Brown, C. R. *Aust. J. Chem.*, **1998**, *51*, 599-604
- (19) Li, J. R.; Li, B. F.; Li, X. C.; Tang, J.; Jiang, L. *Thin Solid Films*, **1996**, *287*, 244-251
- (20) Chen, H.; Herkstoeter, W. G.; Perlstein, J.; Law, K. Y.; Whitten, D. G. *J. Phys. Chem.*, **1994**, *98*, 5138-5146
- (21) Furuki, M.; Pu, L. S.; Sasaki, F.; Yaschi, S. B.; Tani, T. *Mol. Cryst. Liq. Cryst.*, **1998**, *326*, 67
- (22) Tatsuura, S.; Tian, M.; Furuki, M.; Sato, Y.; Sun, L.; Wada, O. *Jpn. J. Appl. Phys.*, **2000**, *39*, 4782-4785
- (23) Tsuchikawa, R.; Ahn, H. A.; S. Yoa; S., Belfield, K.; Ishigami, M. *J. Phys.: Condens. Matter*, **2011**, *23*, 202204 (5pp)
- (24) Sprenger, H. E., Zeigenbein, W. *Angew. Chem. Int. Ed. Engl.* **1967**, *6*, 533-554
- (25) Tian, M.; Kuruki, M.; Iwasa, I.; Sato, Y.; Pu, L.; Tatsuura, S. *J. Phys. Chem. B*, **2002**, *106*, 4370-4376
- (26) Kazmaier, P.; Hamer, G. K.; Burt, R. A. *Can. J. Chem.*, **1990**, *68*, 530
- (27) Law, K. Y.; Bailey, F. C.; Bluett, L. J. *Can. J. Chem.*, **1986**, *64*, 1607
- (28) Hu, L.; Yan, Z.; Xu, H. *RSC Adv.*, **2013**, *3*, 7667-7676

- (29) Dirk, C. W.; Herndon, W. C.; Cervante-Lee, F.; Selnau, H.; Martinez, S.; Kalamegham, P.; Tan, A.; Campos, G.; Velez, M.; Zyss, J.; Ledoux, I.; Chang, L. *J. Am. Chem. Soc.*, **1995**, *117*, 2214-2225
- (30) Chen, G.; Sasabe, H.; Sasaki, Y.; Katagiri, H.; Wang, X.; Sano, T.; Hong, Z.; Yang, Y.; Kido, J. *Chem. Mater.*, **2014**, *26*, 1356-1364
- (31) Jelly, E. E., *Nature*, **1936**, *138*, 1009-1010
- (32) Scheibe, G., *Angew. Chem.*, **1936**, *49*, 563
- (33) Scheibe, G., *Angew. Chem.*, **1937**, *50*, 212-219
- (34) Wurthener, F.; Kaiser, T. E.; Saha-Miller, C. R., *Angew. Chem. Int. Ed.*, **2011**, *50*, 3376-3410
- (35) Hertz, A. H. *Adv. Colloid Interface Sci.*, **1977**, *8*, 237-298
- (36) Kobayashi, T. *J-aggregate*, World Scientific, Singapore, **1996**
- (37) Egorov, V. V. *J. Chem. Phys.*, **2002**, *116*, 3090-3103
- (38) Fidler, H.; Knoester, J.; Wiersma, D. A. *J. Chem. Phys.*, **1991**, *95*, 7880-7890
- (39) Walczak, P. B.; Eisfeld, A.; Briggs, J. S. *J. Chem. Phys.*, **2008**, *128*, 044505 (1-12)
- (40) Hertz, A. H. *Photogr. Sci. Eng.*, **1974**, *18*, 323-335
- (41) von Berlepsch, H.; Bottcher, C. *J. Phys. Chem. B*, **2002**, *106*, 3146-3150
- (42) Kronenberg, N. K.; Meerholz, K. *Chem. Commun.*, **2008**, 6489-6491
- (43) Burckstummer, H.; Kronenberg, N. M.; Gsanger, M.; Stolte, M.; Meerholz, K.; Wurthner, F. *J. Mater. Chem.* **2010**, *20*, 240 – 243
- (44) Silvestri, F.; Irwin, M. D.; Beverina, L.; Facchetti, A.; Pagani, G. A.; Marks, T. J. *J. Am. Chem. Soc.* **2008**, *130*, 17640 – 17641

- (45) Czikkely, V; Forsterling, H. D.; Kuhn, H. *Chemical Physics Letters*, **1970**, 6, 207-210
- (46) McRae, E. G.; Kasha, M. *J. Chem. Phys.*, **1958**, 28, 721-722
- (47) Kasha, M.; El-Bayoumi, M.A.; Rhodes, W. *J. chem. Phys.*, **1962**, 58, 916
- (48) Kasha, M.; Rawls, H. R.; El-Bayoumi, M. A. *Pure Appl. Chem.*, **1965**, 11, 371-392
- (49) Tani, T. *J-Aggregates*; Kabayashi, T., Ed.; World Scientific Publishing: Singapore, **1996**; P 209-228.
- (50) Scherer, P. O. J. *J-Aggregates*; Kabayashi, T., Ed.; World Scientific Publishing: Singapore, **1996**; P 95-110.
- (51) Knoester, J.; Spano, F. C. *J-Aggregates*; Kabayashi, T., Ed.; World Scientific Publishing: Singapore, **1996**; P 111-160.
- (52) Law, K-Y. *J. Phys. Chem.*, **1986**, 91, 5184-5193
- (53) Bello, K. A.; Ajayi, J. O. *Dyes and Pigments*, **1996**, 31, 79-87
- (54) Gsanger, M; Kirchner, E.; Stolte, M.; Burschka, C.; Stepanenko, V.; Pflaum, J.; Wurthner, F. *J. Am. Chem. Soc.*, **2014**, 136, 2351-2362
- (55) Loutfy, R.O.; Hsiao, C. K.; Kazmaier, P. M. *Photogr. Sci. Eng.*, **1983**, 27, 5
- (56) Law, K.Y. *Chem. Rev.*, **1993**, 93, 449
- (57) Alex, S.; Santhosh, U.; Das, S. *J. photochem. Photobiol.*, A **2005**, 172, 63
- (58) Ashwell, G. J. *J. Mater. Chem.*, **1993**, 8, 373
- (59) Kobayashi, T., Ed. *J-Aggregates*, World Publishing Scientific: Singapore, **1996**
- (60) Alex, S.; Basheer, M. C.; Arun, K. T; Ramaiah, D.; Das, S. *J. Phys. Chem. A*, **2007**, 111, 3230

- (61) Nizamov, S. N.; Barakaeva, M. N.; Kurtaliev, E. N.; Tatarets, A. L.; Patsenker, L. D. *Journal of applied Spectroscopy*, **2009**, 76, 464
- (62) Li, J.; Li, B.; Xing-chag Li, X.; Tang, J.; Jiang, L. *Thin Solid Films*, **1996**, 287, 247
- (63) Fukuri, M.; Py, L. S.; Sasaki, F.; Yaschi, S. B.; Tani, T. *Mol. Cryst. Liq. Cryst.*, **1998**, 326, 67
- (64) Tatsuura, S.; Tian, M.; Fukuri, M.; Sato, Y.; Sun. L.; Wada, O. *Jpn. J. Appl. Phys.*, **2000**, 39, 4782
- (65) Tsuchikawa, R.; Ahn, H. A.; S. Yoa, S.; Belfield, K.; Ishigami, M. *J. Phys. Condens. Matter*, **2011**, 23, 202204.
- (66) Tatsuura, S.; Wada, O.; Tian, M.; Fukuri, M.; Sato, Y.; Iwasa, I.; Sun, L.; Kawashima, H. *Applied Physics Letters*, **2001**, 79, 2517
- (67) Gorner, H., Slavnova, T. D., Chibisov, A. K. *J. Phys. Chem. B*, **2010**, 114, 9330
- (68) Vujacic, A.; Vasic, V.; Dramicanin, M.; Sovilj, S. P.; Bibic, N.; Hranisavljevic, J.; Wiederrecht, G. *J. Phys. Chem. C*, **2012**, 116, 4655-4661
- (69) Lewis, E. S. *Investigation of Rates and Mechanisms of Reaction*, Wiley-Interscience : New York, **1974**; 758
- (70) Moshino, H.; Hasegawa, S.; Mouri, S.; Miura, Y. F.; Sugi, M. *Jpn. J. Appl. Phys.*, **2008**, 47, 1034-1041
- (71) Li, G.; Zhu, R.; Yang, Y. *Nature Photonics*, **2012**, 6, 153-161
- (72) Spencer, S. D.; Bougher, C.; Heaphy, P. J.; Muricia, V. M.; Gallivan, C. P.; Monfett, A.; Anderson, J. D.; Lody, J.A. ; Conrad, B. R.; Collison, C. J. *Solar Energy Materials and Solar Cells*, **2013**, 112, 202-208

- (73) Chen, G.; Sasabe, H.; Lu, W.; Wang, X.; Kido, J.; Hong, Z.; Yang, Y. *Mater. Chem. C*, **2013**, *1*, 6547-6552
- (74) Spencer, S.; Hu, H.; Li, Q.; Ahn, H. Y.; Quaddoura, M.; Yao, S.; Laonnidis, A.; Belfield, B.; Collison, C. J. *Prog. Photovolt: Res. Appl.*, **2014**, *22*, 488-493